CASE FILE
COPY

TECHNICAL NOTES

NATIONAL ADVISORY COMMITTEE FOR AERONAUTICS

No. 541

THE EFFECT OF THE ANGLE OF AFTERBODY KEEL ON

THE WATER PERFORMANCE OF A FLYING-BOAT HULL MODEL

By John M. Allison
Langley Memorial Aeronautical Laboratory

Washington
September 1935

NATIONAL ADVISORY COMMITTEE FOR AERONAUTICS

E R R A T A

TECHNICAL NOTE NO. 541

THE EFFECT OF THE ANGLE OF AFTERBODY KEEL ON

THE WATER PERFORMANCE OF A FLYING-BOAT HULL MODEL

Page 7, second line from bottom:

"Take-off time, sec.   27.2   28.4   28.7   35.7 --"

should read

"Take-off time, sec.   54.4   56.8   57.4   71.4 --"

NATIONAL ADVISORY COMMITTEE FOR AERONAUTICS

TECHNICAL NOTE NO. 541

THE EFFECT OF THE ANGLE OF AFTERBODY KEEL ON

THE WATER PERFORMANCE OF A FLYING-BOAT HULL MODEL

By John M. Allison

SUMMARY

N.A.C.A. model 11-C was tested in the N.A.C.A. tank
according to the general method with the angle of after-
body keel set at five different angles from 2-1/2° to 9°,
but without changing other features of the hull. The re-
sults of the tests are expressed in curves of test data
and of nondimensional coefficients.

At the depth of step used in the tests, 3.3 percent
beam, the smaller angles of afterbody keel give greater
load-resistance ratios at the hump speed and smaller at
high speed than the larger angles of afterbody keel. Com-
parisons are made of the load-resistance ratios at several
other points in the speed range.

The effect of variation of the angle of afterbody
keel upon the take-off performance of a hypothetical fly-
ing boat of 15,000 pounds gross weight having a hull of
model 11-C lines is calculated, and the calculations show
that the craft with the largest of the angles of after-
body keel tested, 9°, takes off in the least time and dis-
tance.

INTRODUCTION

The afterbody and forebody of the hull of a flying
boat act together to produce the total hydrodynamic lift
and resistance. At rest, and at low speeds, the forebody
and afterbody together supply the buoyancy required to
keep the hull afloat. With increase in speed, the bow
rises and the afterbody surface runs in the water at a
positive angle of attack favorable for lifting. After the
hull rises on the step and planing begins, the afterbody
no longer plays an important part in providing lift, but
it may be a source of considerable resistance if it runs

near enough to the surface of the water to be struck by spray thrown back from the planing forebody.

The general effect of change in the angle of afterbody keel upon the water performance of models of flyingboat hulls had been observed in testing a number of models, but it could not be determined quantitatively in those tests because it could not be separated from the effects of other changes. These tests have been made with a model of generally conventional form in which the angle of afterbody keel can be changed without changing the rest of the model.

DESCRIPTION OF MODEL

N.A.C.A. model 11-C, the offsets for which are given in table I, was used in these tests. As shown in figure 1, this model was made in two pieces joined at the step and was so arranged that the angle of afterbody keel could be changed by inserting wooden wedges of suitable taper between the afterbody and forebody. The angle between the afterbody keel and the base line is taken as the angle of afterbody keel; the angle between the forebody and afterbody keel lines will be 1° more than the angle of afterbody keel, as defined. The distance from the step to the after end of the afterbody, or sternpost, was kept constant for all the changes investigated.

The model was built of laminated mahogany with a tolerance of 0.02 inch on dimensions below the chines. The surface was finished with several coats of gray enamel rubbed smooth. The settings of the angle of afterbody keel are believed to be accurate to $\pm 0.15^{\circ}$. For convenience, each change of setting was given an identification number following the 11-C as follows:

Model	Angle of afterbody keel
11-C-7	$2\text{-}1/2^{\circ}$
11-C-8	4°
11-C	$5\text{-}1/2^{\circ}$
11-C-9	7°
11-C-10	9°

APPARATUS AND TEST METHOD

The N.A.C.A. tank and its equipment used in these tests are described in references 1 and 2. The tests were of the "general" type in which the model is towed at a number of constant speeds at different fixed angles of trim and at different constant loads.

RESULTS

The net values of resistance and trimming moment are plotted against speed in figures 2 to 33 and include the air drag on the part of the model above the water. The center about which moments are taken is shown in figure 1. A positive trimming moment is one that tends to increase the trim angle; that is, to raise the bow. Trim angle in this case is the angle between the base line and the water surface.

Precision.- The test results as represented by the faired curves are believed to be accurate within the following limits:

Resistance	±0.2 lb.
Load	± .3 lb.
Speed	± .1 ft./sec.
Trim angle	± .1°
Trimming moment	±1 lb.-ft.

Derived data.- The nondimensional coefficients used are as follows:

Speed coefficient, $C_V = \dfrac{V}{\sqrt{gb}}$

Resistance coefficient, $C_R = \dfrac{R}{wb^3}$

Load coefficient, $C_\Delta = \dfrac{\Delta}{wb^3}$

Trimming-moment coefficient, $C_M = \dfrac{M}{wb^4}$

where Δ is load on water, lb.

      R,   water resistance, lb.

      M,   trimming moment, lb.-ft.

      w,   specific weight of water (63.5 lb. per cu.ft.
         for water in the N.A.C.A. tank).

      g,   acceleration of gravity, ft./sec.^{2}

      b,   beam of hull, ft.

      V,   speed, ft./sec.

These coefficients may be used with any consistent system of units.

Figures 34 to 38, in which C_R is plotted against C_V at best trim angle τ_o, with C_Δ as a parameter, are developed from the original resistance curves by cross-plotting. The points for the Δ/R curves of figure 39 are calculated directly from figures 34 to 38. The maximum trimming-moment coefficient curves of figure 41 are obtained from the maximum positive values of trimming moment for each angle and load in figures 2 to 32.

<div align="center">DISCUSSION</div>

Resistance characteristics.- In figure 39, the load-resistance ratio Δ/R is plotted against C_Δ for each angle of afterbody keel with the values of the parameter C_V chosen to bring out a performance comparison at various speeds. Figure 40 presents the same information but with Δ/R plotted against angle of afterbody keel. At hump speed, Δ/R decreases with increase in angle of afterbody keel. The percentage decrease is greater for the larger values of C_Δ. At $C_V = 4.5$ and $C_V = 6.0$, large improvement is obtained by increasing the angle of afterbody keel from 2-1/2° to 5-1/2°. Any further increase produces a much smaller improvement. At $C_V = 3.5$, which is intermediate between hump and high speeds, the small angles of afterbody keel have the best values of Δ/R, but the trend is less marked than at hump speed.

The increase in Δ/R ratio at the hump speed resulting from a decrease in angle of afterbody keel probably results from the additional lift given by the afterbody surface running at a more favorable angle of attack. This additional lift helps raise the hull out of the water, thus decreasing the wave-making resistance.

At speed coefficients of 4.5 and 6.0 the forebody carries practically all of the load while the afterbody contributes only frictional resistance; high angles of afterbody keel result in higher Δ/R ratios because they reduce the area of afterbody surface struck by water coming from the step.

Trimming-moment characteristics.- The large lift produced by an afterbody bottom surface running at a high angle of attack causes the center of pressure of the water forces to move aft. Consequently, the smaller the angle of afterbody keel, the greater the angle of attack of the afterbottom surface for a given trim and the farther aft the center of pressure will move. For example, in the curves for $\tau = 9°$ and $\tau = 11°$ (fig. 41) the center of pressure has moved so far aft that the maximum moment is negative for all loads.

Trim-angle characteristics.- The best trim angle at the hump decreases but slightly in magnitude with decrease in angle of afterbody keel. At high speeds, reducing the angle of keel appreciably decreases the best trim angle. The difference in best trim angle between two of these hulls is, however, numerically less than the difference in their angles of afterbody keels. Therefore the afterbody of small keel angles will run closer to the surface of the water.

Static characteristics.- Figures 42 and 43 are plotted from test data. In figure 42, the trimming moments at rest are plotted for the various settings of angle of afterbody keel. These curves are useful for estimating the magnitude of the effect of a change in angle of afterbody keel upon the attitude at rest of a hull of this type. The center of moments used was that shown on figure 1. Figure 43 consists of curves showing the drafts at rest of each model for different trim angles and loads. The smaller the angle of afterbody keel, the higher in the water the hull will tend to float owing to the buoyancy supplied by the afterbody.

Spray characteristics and general behavior.- The photographs of the models running in the water show that the spray characteristics are affected by changes in the angle of afterbody keel. The effect is shown in the enlarged photographs (figs. 44(a) to 44(d)), which compare model 11-C-10 (9° angle of afterbody keel) and 11-C-8 (4° angle of afterbody keel) at the same trim angle (7°) and load, and at approximately the same speed. When comparing the pictures of the bow (c) and (d), it will be observed that the bow wave in (c) (9° angle of afterbody keel) is considerably higher than that in (d) (4° angle of afterbody keel). Drafts observed at this speed (slightly below hump speed) show the model in (c) to be riding deeper in the water than the one in (d). The resistances were 22.9 pounds for model 11-C-10, shown in 44(c) and 18.9 pounds for model 11-C-8, shown in 44(d). Pictures of the sterns of the same models under the same conditions are shown in 44(a) and 44(b), respectively. The afterbody of the model in (b) is running at a larger angle of attack and producing more lift than the one in (a) as evidenced in the photograph by the heavier waves at the stern. The bow wave of the model with 9° angle of afterbody keel (c) is slightly higher than that of the model with 4° angle of afterbody keel (d), thereby verifying the condition observed when comparing (c) and (d). The photographs in figures 45(a) and 45(b) furnish a basis for the comparison of the same models running at 9° angle of trim, 40 pounds load, and slightly above hump speed. Model 11-C-10 shown in 45(a) with the larger angle of afterbody keel has its afterbody clear of the water while the one in 45(b) 11-C-8, does not. The resistances were 8.8 pounds and 9.3 pounds, respectively.

Riding on the afterbody occurred during the testing of model 11-C-7 (2-1/2° angle of afterbody keel). In this attitude the step is entirely out of the water. The dotted line on the resistance curve for a load of 5 pounds (fig. 6) shows how the resistance drops, beginning at a speed of 35 feet per second. At a trim angle of 7° and loads of 20 and 40 pounds, this model rode on the afterbody at all speeds above 25 feet per second. A full-scale hull of a flying boat could not be made to ride on the afterbody because the control moment required to hold the attitude would be too great.

Take-off example.- The effect of changing the angle of the afterbody keel can be seen from the following example. A hypothetical flying boat is assumed to be fitted

successively with five hulls each similar to one of the
model 11-C forms that were tested. Aside from the hull
each combination has the following characteristics:

        Gross load . . . . 15,000 lb.

        Wing area   . . . . 1,000 sq.ft.

        Horsepower (two engines) . . . 1,240

        Effective aspect ratio
           (with ground effect) 7.0

        Parasite-drag coefficient
           (excluding hull) 0.05

        Airfoil . . . . Clark Y (data taken
                                          from T.R. No. 352,
                                          N.A.C.A.)

        Propeller diameter . . . . .   10 ft.

        Propeller pitch angle
           (fixed pitch at 0.75R) . . . 19°

     A wing setting of 8° was used in all cases in order
quickly to transfer the load from the hull to the wings.
The curves for thrust, total resistance (air plus water),
and air drag are shown in figure 46. The thrust was cal-
culated from the charts of reference 3.

     The calculated performances of the flying boats com-
pare as follows:

Hull	11-C-10	11-C-9	11-C	11-C-8	11-C-7
Angle of after-body keel, deg.	9	7	5-1/2	4	2-1/2
Beam, ft.	8.075	8.075	8.075	8.075	8.075
Take-off time, sec.	27.2	28.4	28.7	35.7	--
Take-off run, ft.	3460	3640	3830	5140	--

It will be seen that at a speed of 85 feet per second the resistance of the craft with the 2-1/2° angle of afterbody keel exceeds the thrust and does not fall below the thrust until a speed of 95 feet per second is reached. With this hull the craft will not take off.

The tabulated values of take-off time and distance indicate that little additional improvement can be expected by increasing the angle of afterbody keel beyond 9°.

Figure 46 shows that setting the afterbody of the hypothetical hull at a small angle causes a decrease in excess thrust that extends over a considerable portion of the high-speed range; whereas, the gain in excess thrust at the hump extends over a small range of speed. If larger thrust had been assumed, the high-speed resistance peak would have been less critical and the advantage shown by the larger angles of afterbody keel would have been reduced.

CONCLUSIONS

These conclusions are based on tests of models having a depth of step of 3.3 percent of the beam. Changing the depth of the step will produce effects that were not present in these tests.

1. A small angle of afterbody keel is favorable for low resistance at low speed and a large angle is best at high speeds.

2. For the hull tested, having a load coefficient C_Δ of 0.4 at the hump, the optimum angle of afterbody keel is near 9°.

3. A small angle of afterbody keel reduces the maximum positive trimming moment.

4. A hull with a large angle of afterbody keel has a larger best trim angle at high speeds.

Further tests are planned in which the angle of afterbody keel will be varied up to 15° for each of several depths of step.

Langley Memorial Aeronautical Laboratory,
      National Advisory Committee for Aeronautics,
            Langley Field, Va., July 10, 1935.

REFERENCES

1. Truscott, Starr: The N.A.C.A. Tank - A High Speed
   Towing Basin for Testing Models of Seaplane Floats.
   T.R. 470, N.A.C.A., 1933.

2. Shoemaker, James M.: Tank Tests of Flat and V-Bottom
   Planing Surfaces. T.N. No. 509, N.A.C.A., 1934.

3. Hartman, Edwin P.: Working Charts for the Determina-
   tion of Propeller Thrust at Various Air Speeds.
   T.R. No. 481, 1934.

TABLE I

Offsets for N.A.C.A. Model No. 11-C Flying-Boat Hull (Inches)

Station	Distance from F.P.	Distance from base line									Half breadths								Station
		Keel	B1 1.50[1]	B2 3.00	B3 4.50	B4 6.00	B5 7.50	Main chine	Cove	Upper chine	Main chine	Cove	Upper chine	WL1 12.50[2]	WL2 11.00	WL3 9.50	WL4 8.00	WL5 6.50	
F.P.	0.0	4.00						4.00			0.15								F.P.
1/2	2.4	9.17	5.90					5.29			2.07						0.52	1.16	1/2
1	4.8	10.85	8.20	6.64				6.34			3.53					0.73	1.64	3.22	1
1-1/2	7.2	11.87	9.72	8.12				7.18			4.67				0.64	1.67	3.15		1-1/2
2	9.6	12.53	10.76	9.27	7.24			7.87			5.59			0.16	1.30	2.74	5.13		2
3	14.4	13.21	12.01	10.83	8.27			8.89			6.90			.93	3.76	5.10			3
4	19.2	13.47	12.62	11.72	9.83	9.13		9.56			7.71								4
5	24.0	13.58	12.94	12.23	10.91	10.18	9.62	9.97			8.17								5
6	28.8	13.66			11.53	10.85	10.22	10.19			8.40								6
7	33.6	13.75						10.30			8.49								7
8	38.4	13.83						10.38			8.50								8
9	43.2	13.92						10.47			8.50								9
10,F.	48.0	14.00						10.55			8.50								10,F.
10,A.	48.0	13.44						9.98			8.50								10,A.
11	52.8	12.97						9.51	8.29		8.50								11
12	57.6	12.51						9.22	7.63	8.16	8.10	8.10	8.40						12
13	62.4	12.04						9.22	7.27	7.15	6.97	6.97	8.11						13
14	67.2	11.58						9.54	7.27	6.23	5.07	5.07	7.58						14
15	72.0	11.11						10.10	7.17	5.44	2.59	2.59	6.77						15
S.P.	76.0	10.74 *7.24						10.72	7.23		.20	.20							S.P.
16	76.8	7.04								4.71			5.78						16
17	81.6	5.91								4.06			4.61						17
18	86.4	4.77								3.46			3.31						18
19	91.2	3.64								2.91			1.90						19
20	96.0	2.50								2.39			.40						20

Elements of stations — Straight lines from here aft (at station 6).

[1] Distance from center line (plane of symmetry) to buttock (section of hull surface made by a vertical plane parallel to plane of symmetry).

[2] Distance from base line to water line (section of hull surface made by a horizontal plane parallel to base line).

Fig. 1

Figure 1.—Model 11-C Angle of keel variations

Figure 3.- Resistance and trimming moment, $\tau = 2^\circ$, Model 11-0-10 (3-1/2° angle of afterbody keel.)
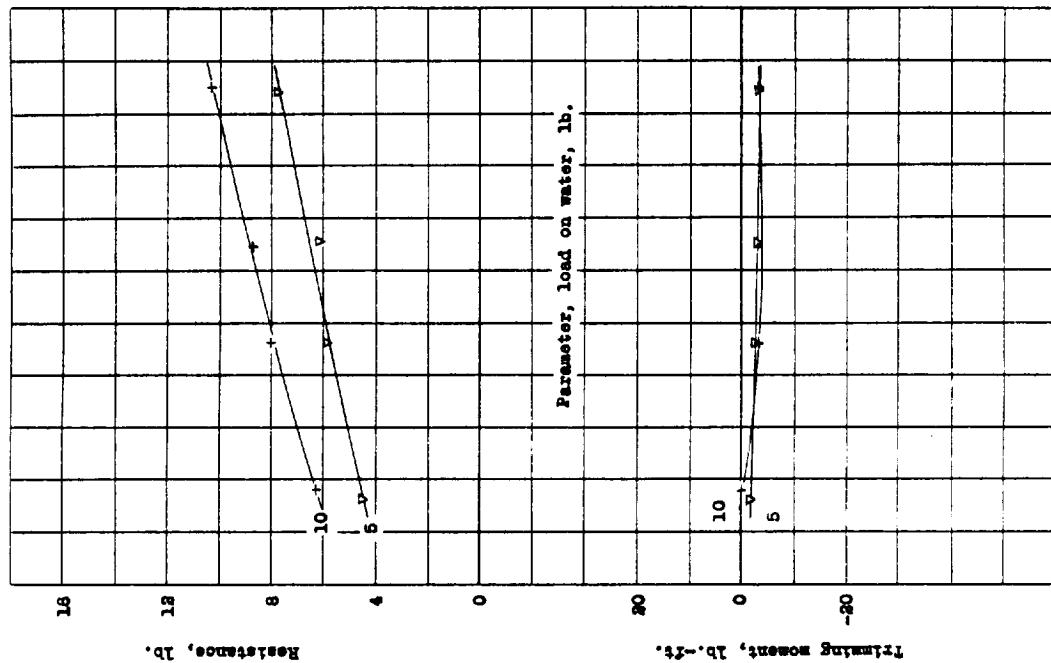
Figure 2.- Resistance and trimming moment, $\tau = 1^\circ$, Model 11-0-7 (3-1/2° angle of afterbody keel.)

Fig. 4
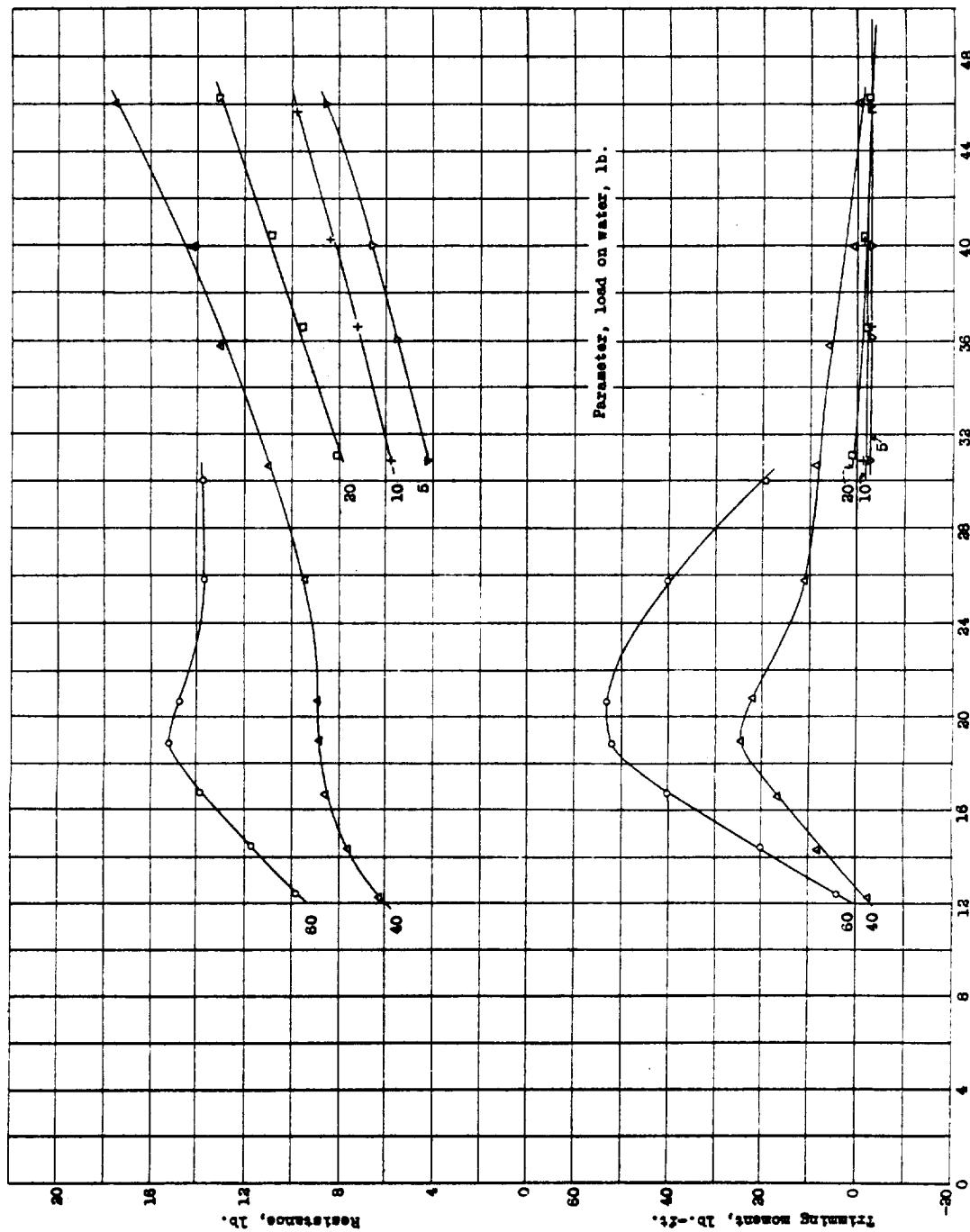


Figure 4.- Resistance and trimming moment, $\tau = 3°$. Model 11-C-7 ($3\text{-}1/2°$ angle of afterbody keel).

Figure 8.- Resistance and trimming moment.(τ = 9°, Model 11-G-7 (2-1/2° angle of afterbody keel.)
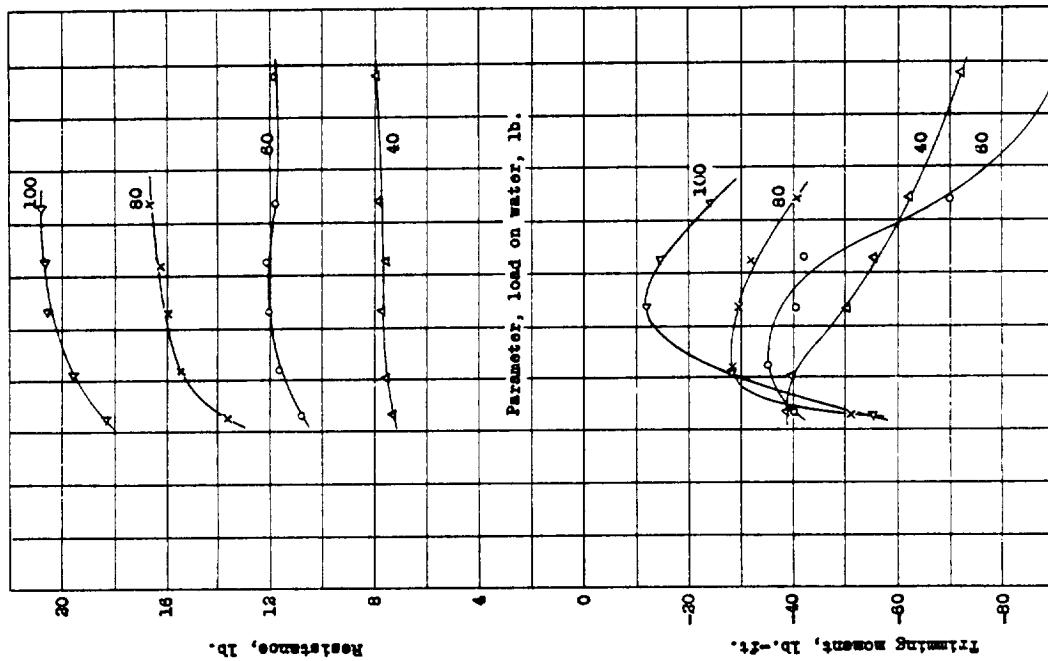
Figure 5.- Resistance and trimming moment.(τ = 4°, Model 11-G-7 (2-1/2° angle of afterbody keel.)

Fig. 6
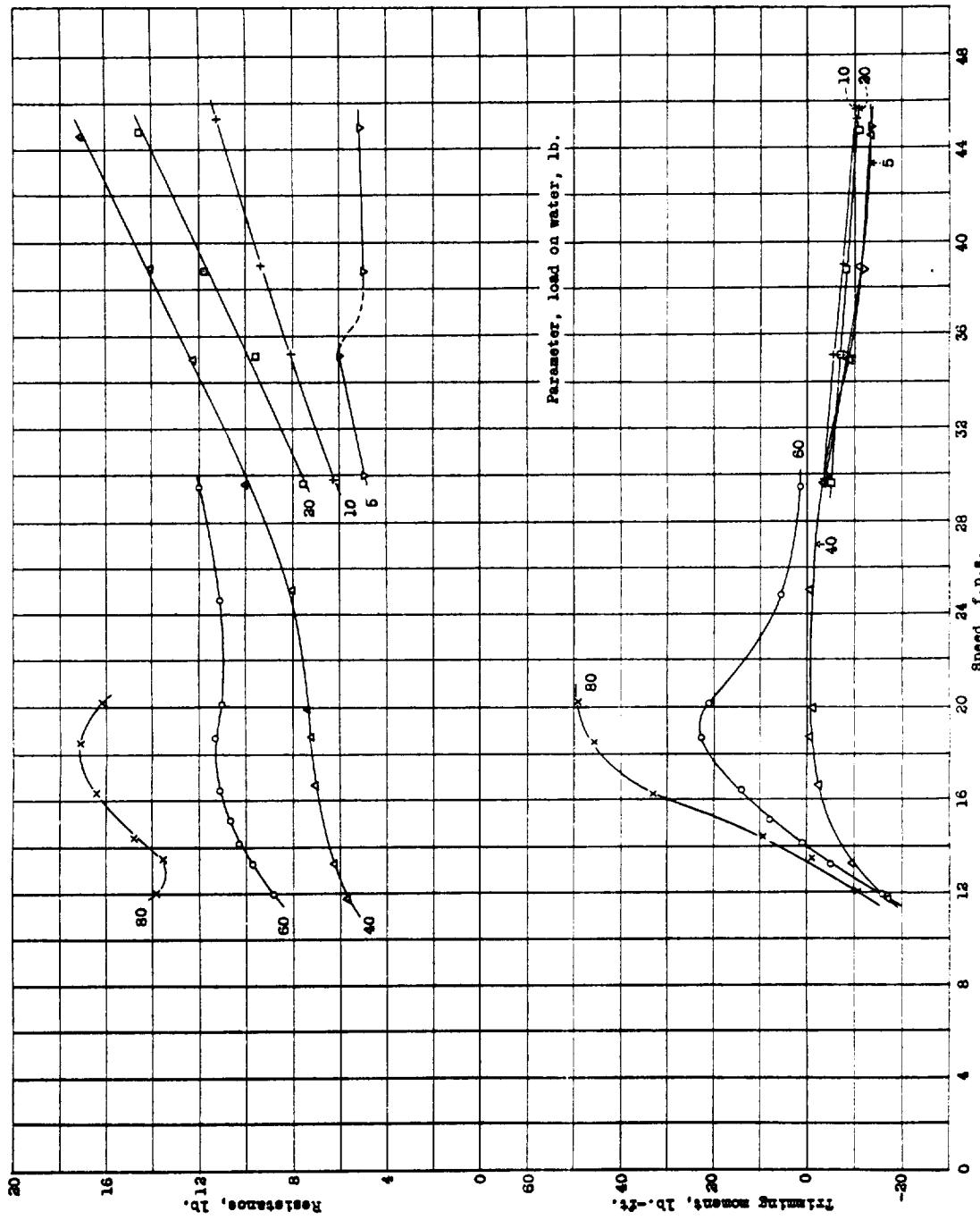
Figure 6.- Resistance and trimming moment, τ = 5°. Model 11-C-7 (2-1/2° angle of afterbody keel).

Fig. 7
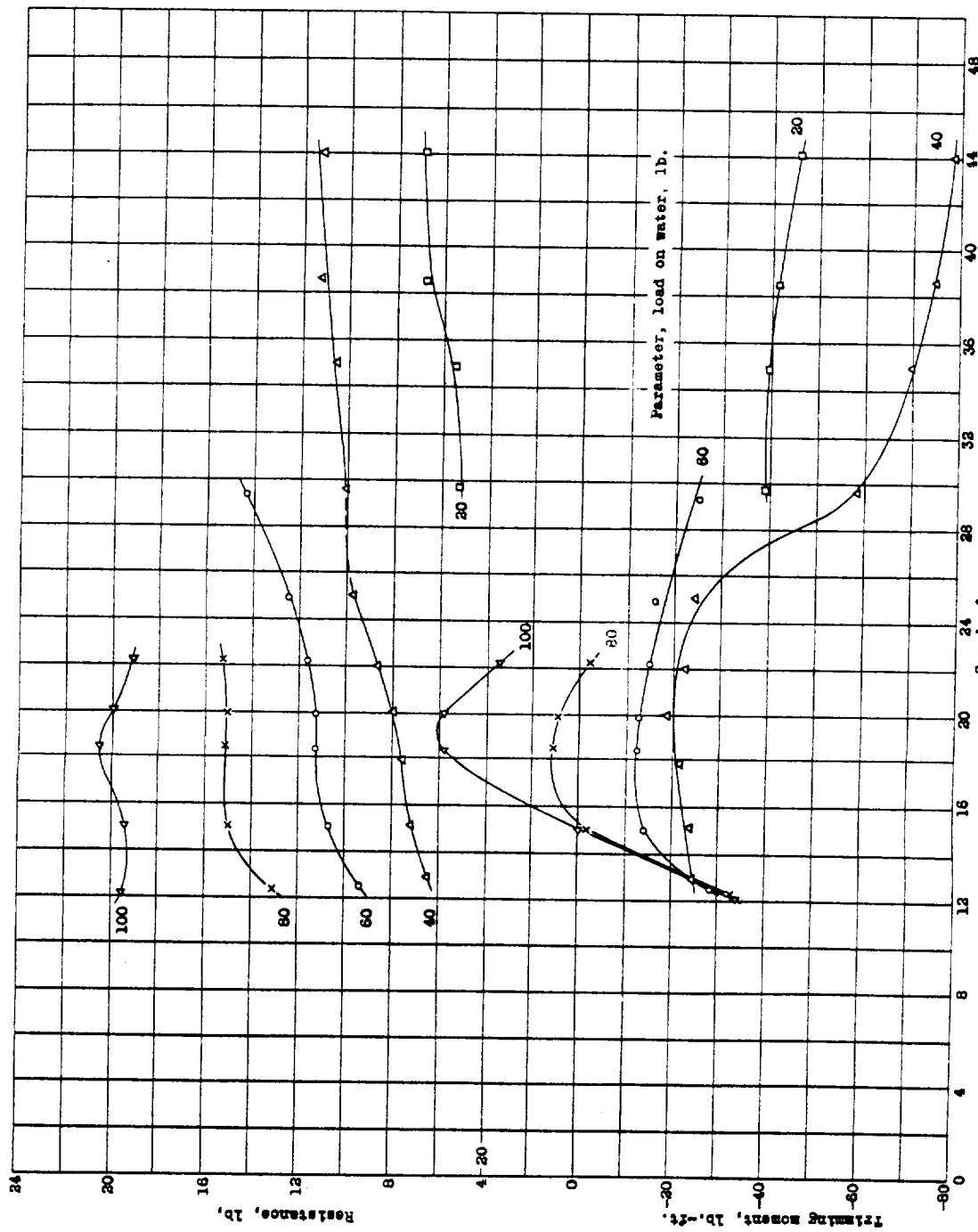
Figure 7.- Resistance and trimming moment, $\tau = 7°$. Model 11-0-7 (3½/2° angle of afterbody keel)

Figure 10.- Resistance and trimming moment, τ = 2°, Model 11-0-8 (4° angle of afterbody keel.)
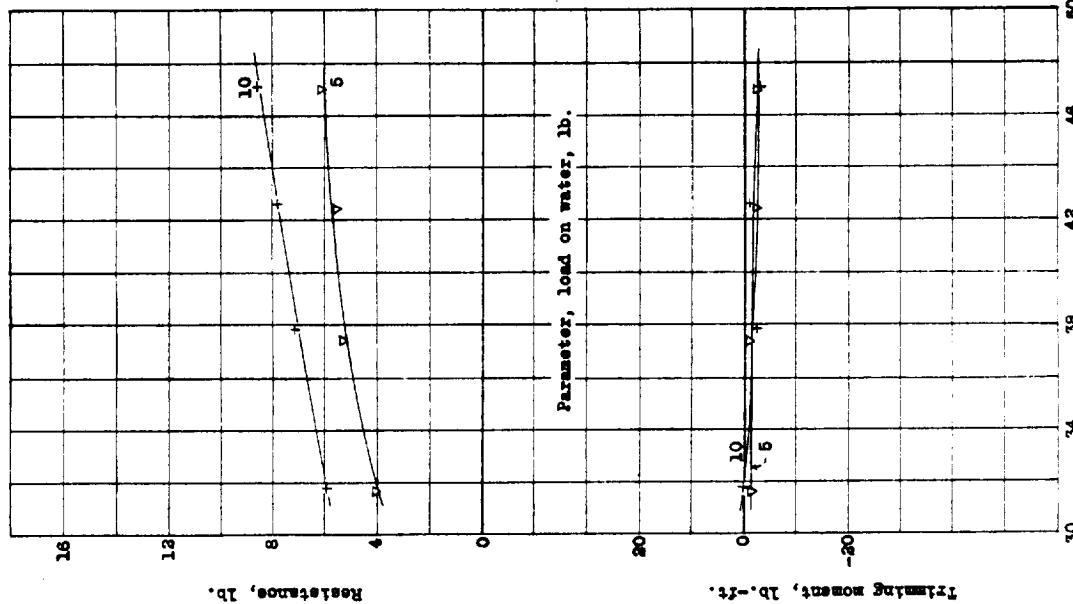
Figure 9.- Resistance and trimming moment, τ = 11°, Model 11-0-7 (2-1/2° angle of afterbody keel.)

Fig. 11
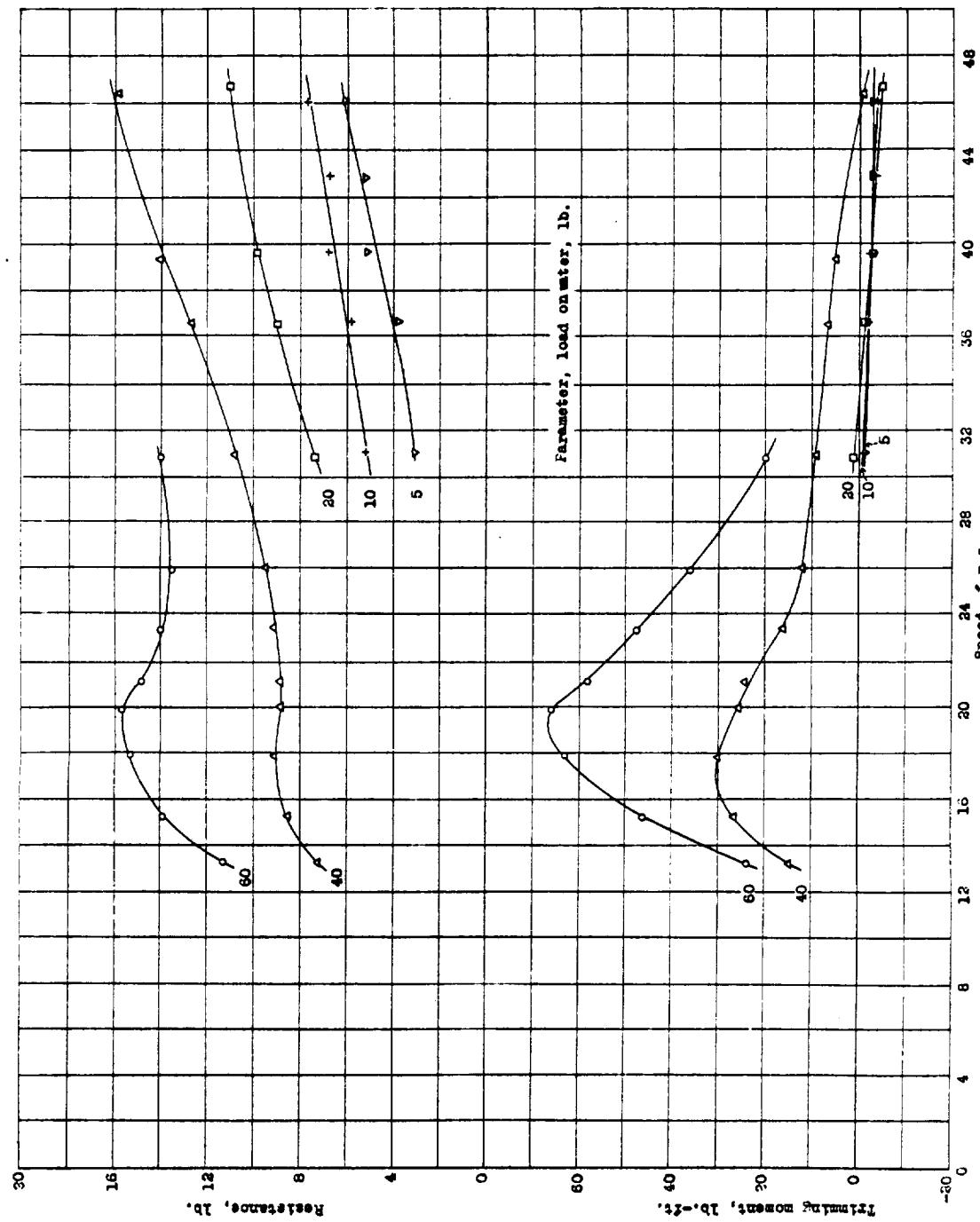
Figure 11.- Resistance and trimming moment, $\tau = 3°$. Model 11-G-8 ($4°$ angle of afterbody keel).

Fig. 12
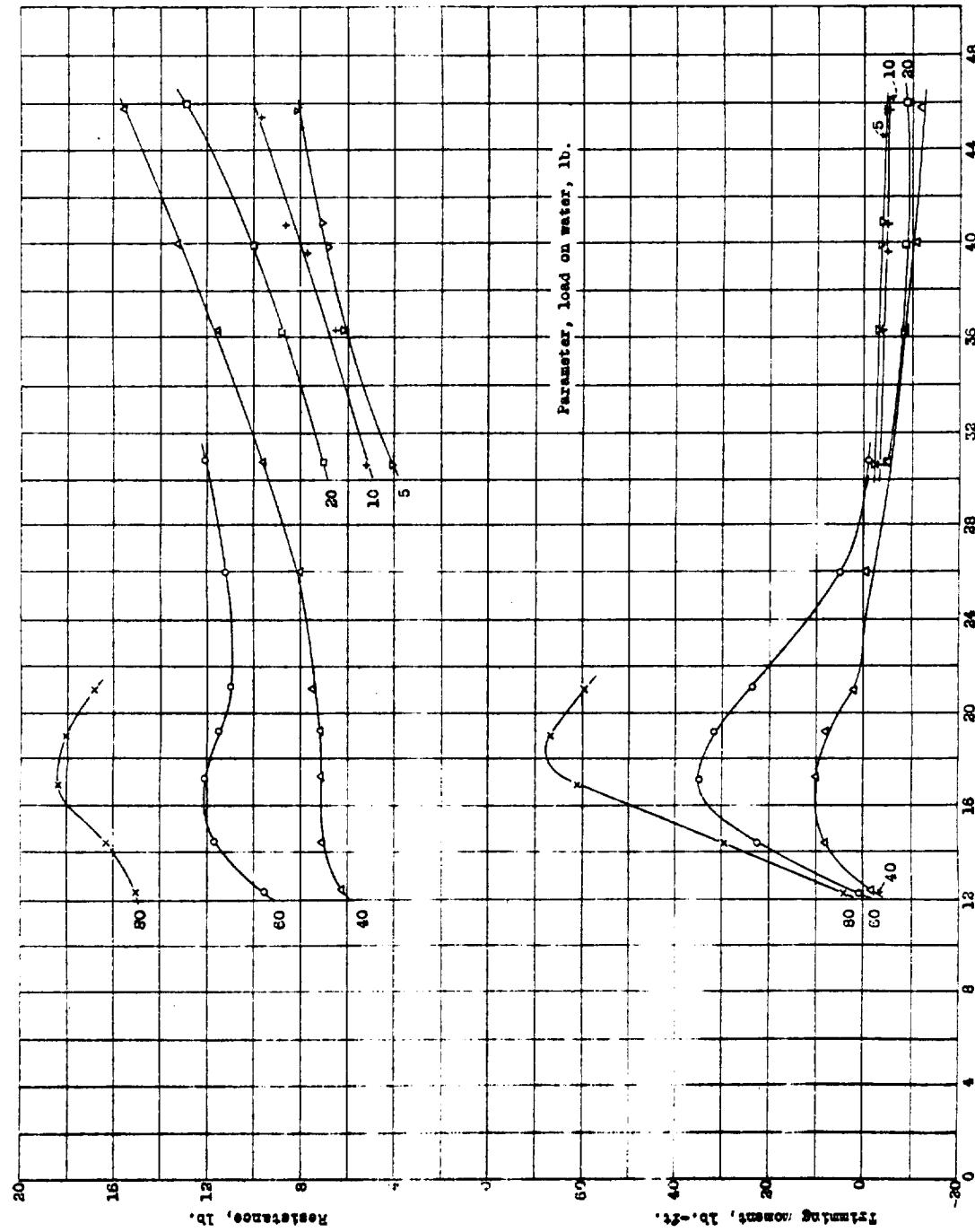
Figure 12.- Resistance and trimming moment, τ = 5°. Model 11-C-8 (4° angle of afterbody keel).

Fig. 13
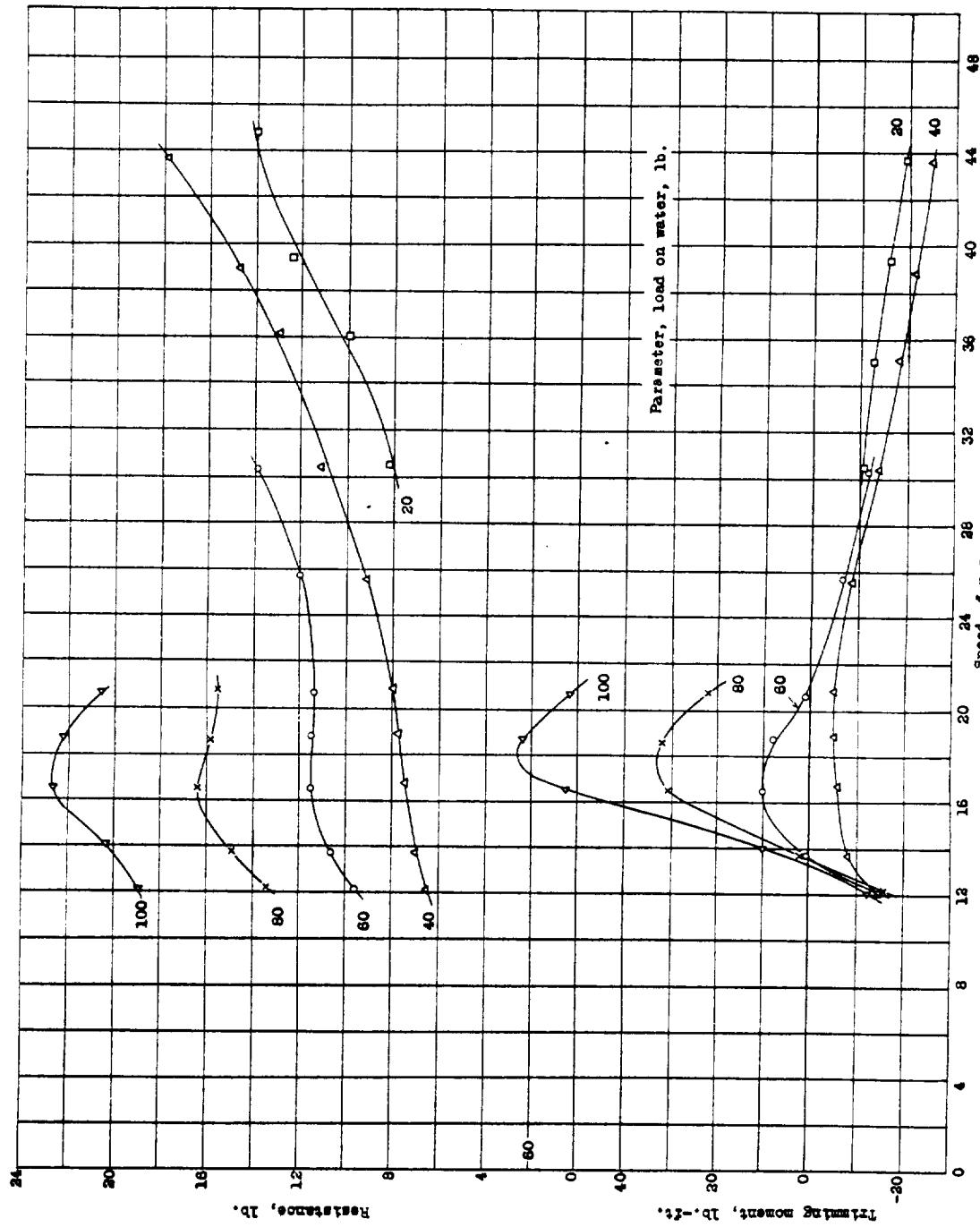

Figure 13.- Resistance and trimming moment, τ = 7°, Model 11-C-8 (4° angle of afterbody keel).
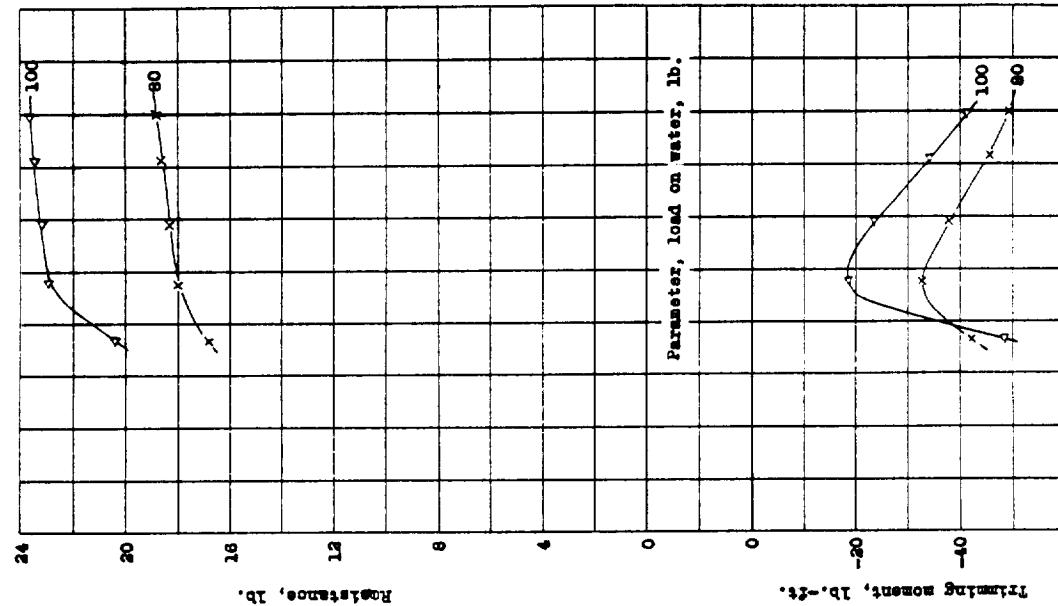
Figure 15.- Resistance and trimming moment, τ = 11°, Model 11-C-8 (4° angle of afterbody keel.)

Figure 14.- Resistance and trimming moment, τ = 9°, Model 11-C-8 (4° angle of afterbody keel.)

Parameter = load on water, lb.
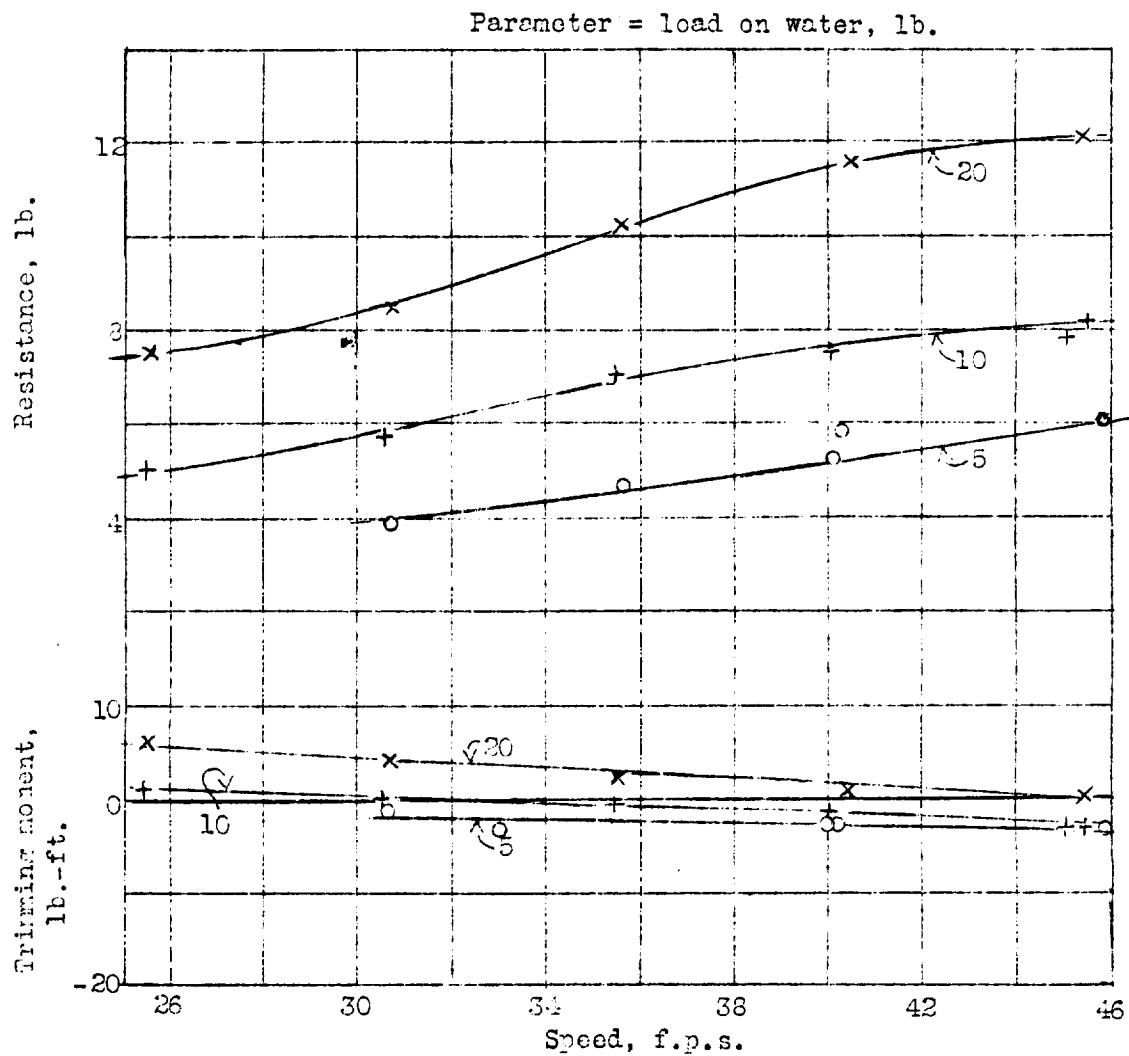
Figure 16 - Resistance and trimming moment, $\tau = 2°$. Model 11-C.
($5\frac{1}{2}°$ angle of afterbody keel).

Fig. 17
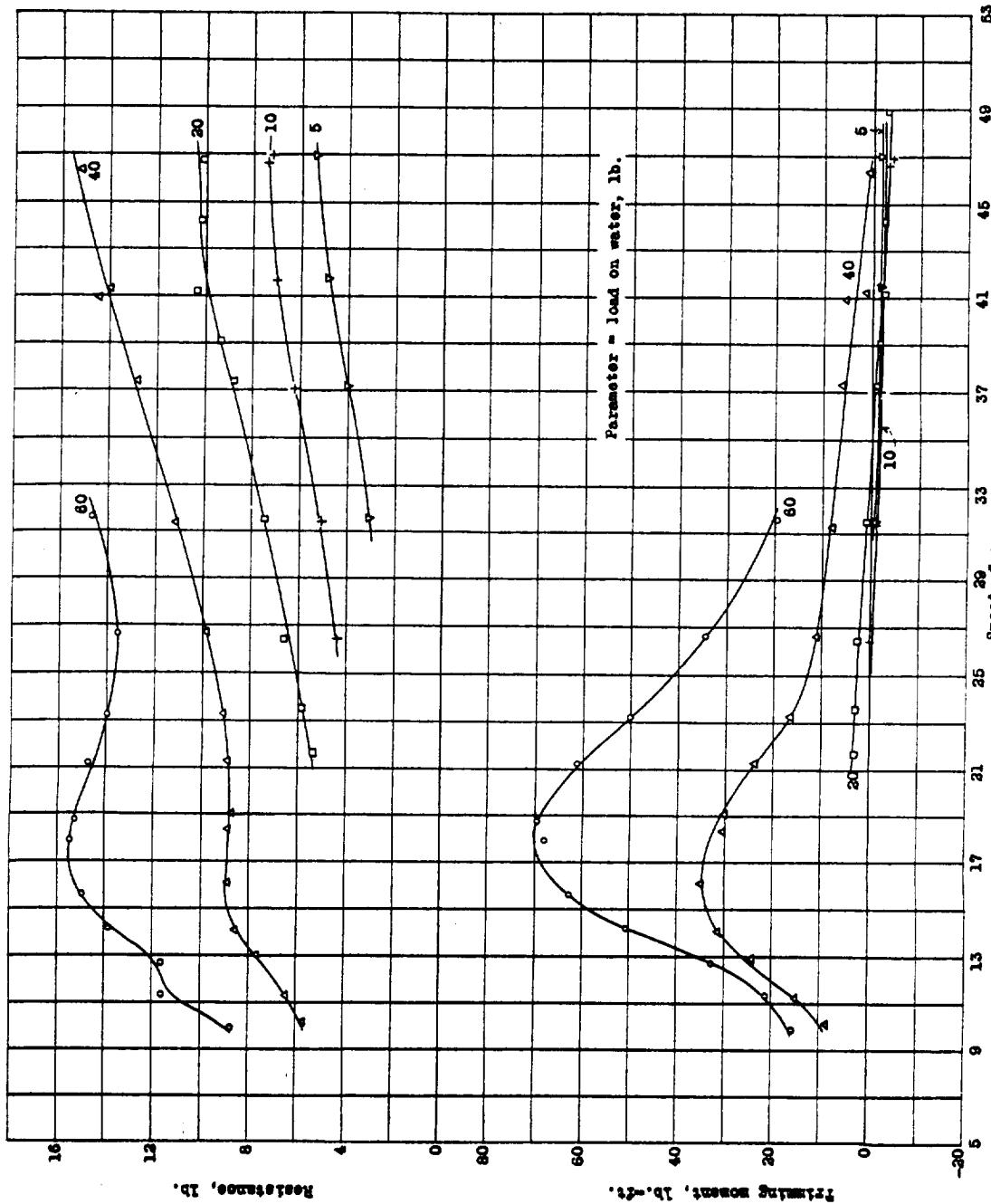
Figure 17.—Resistance and trimming moment. $\tau = 3^\circ$. Model 11-C. ($5\frac{1}{2}^\circ$ angle of afterbody keel)

Fig. 18
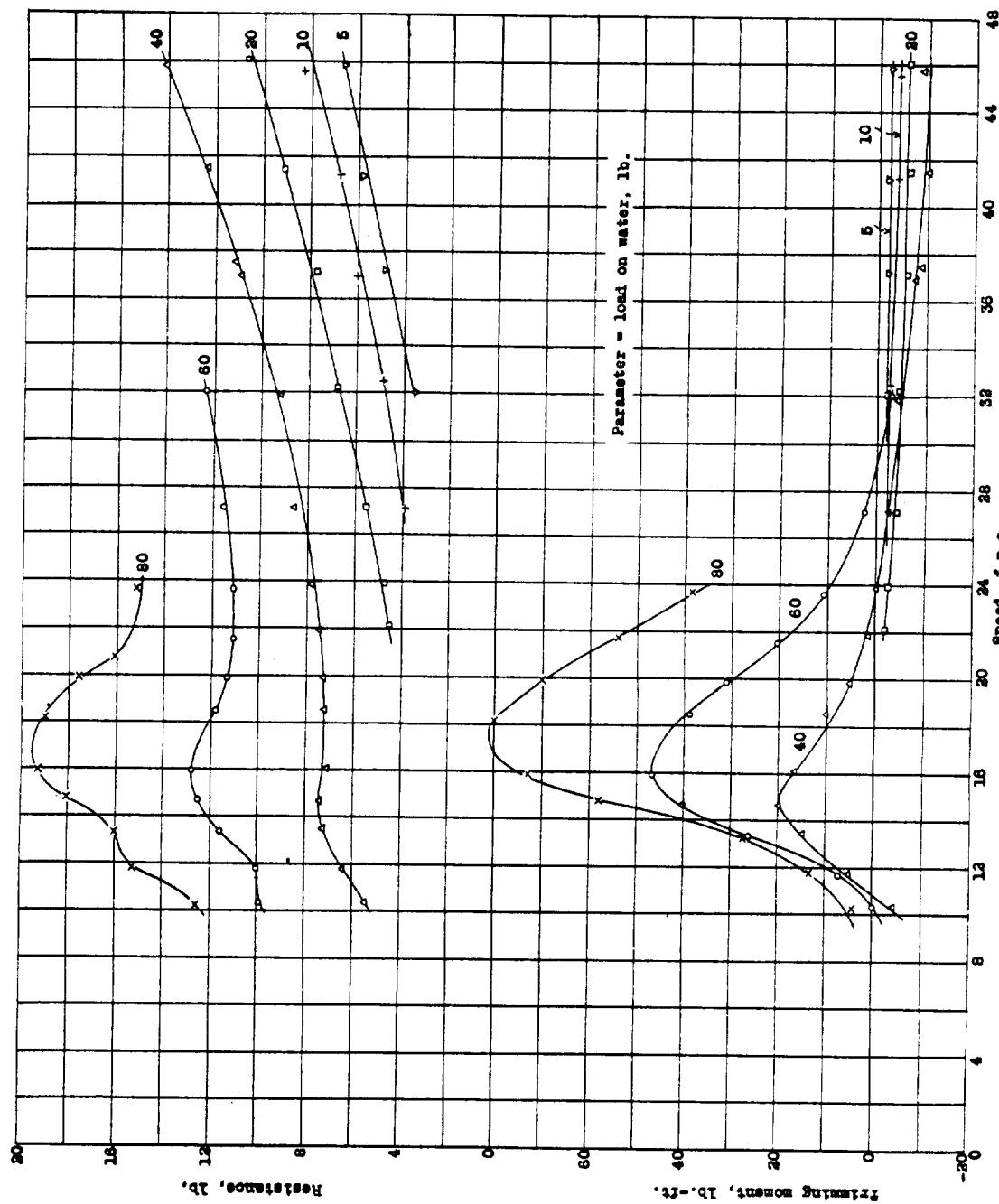
Figure 18.—Resistance and trimming moment. $\tau = 5°$. Model 11-C. ($5\frac{1}{2}°$ angle of afterbody keel)

Parameter = load on water, lb.

Figure 19a.—Resistance. τ = 7°. Model 11-C. (5½° angle of afterbody keel)

Speed, f.p.s.
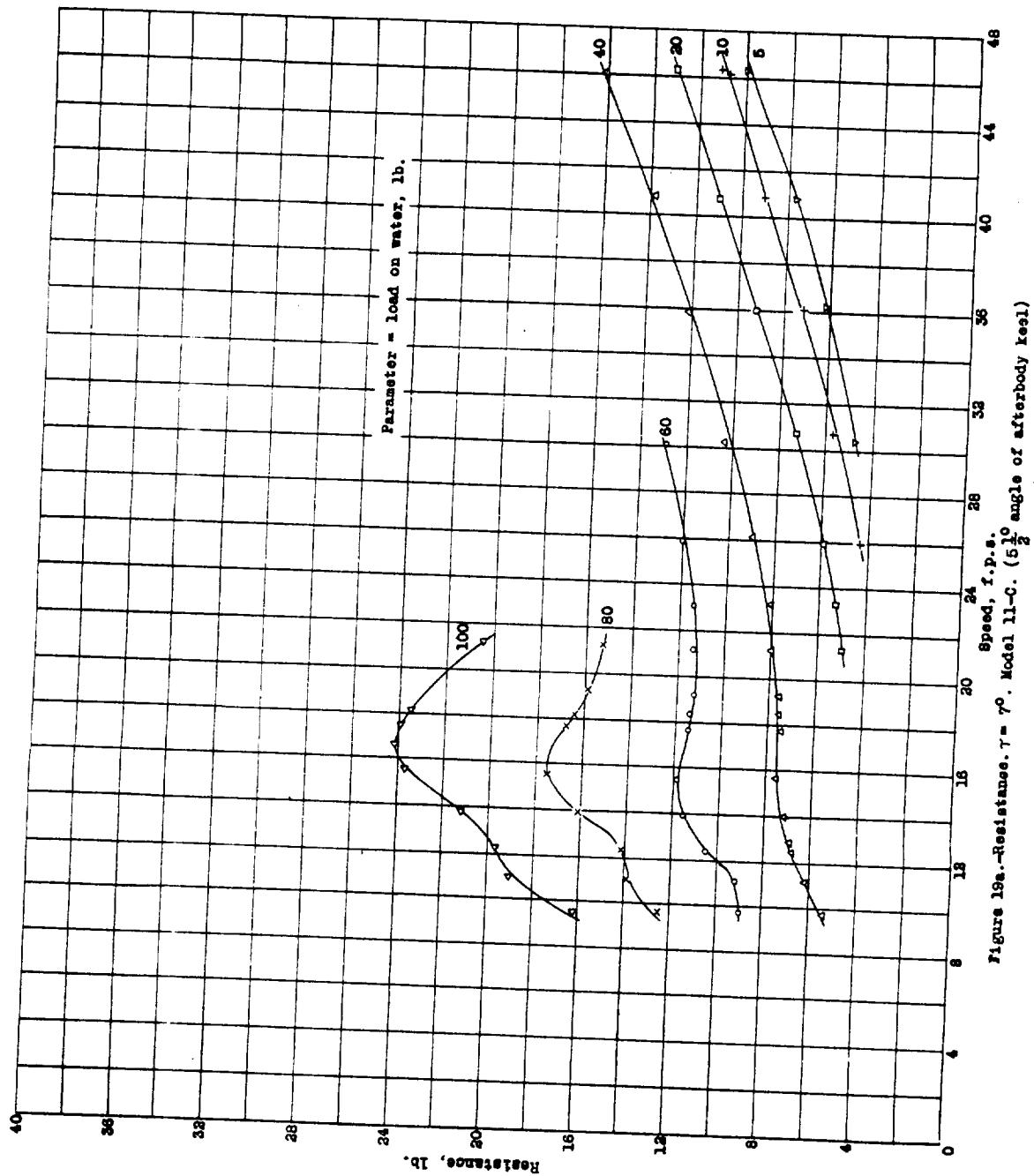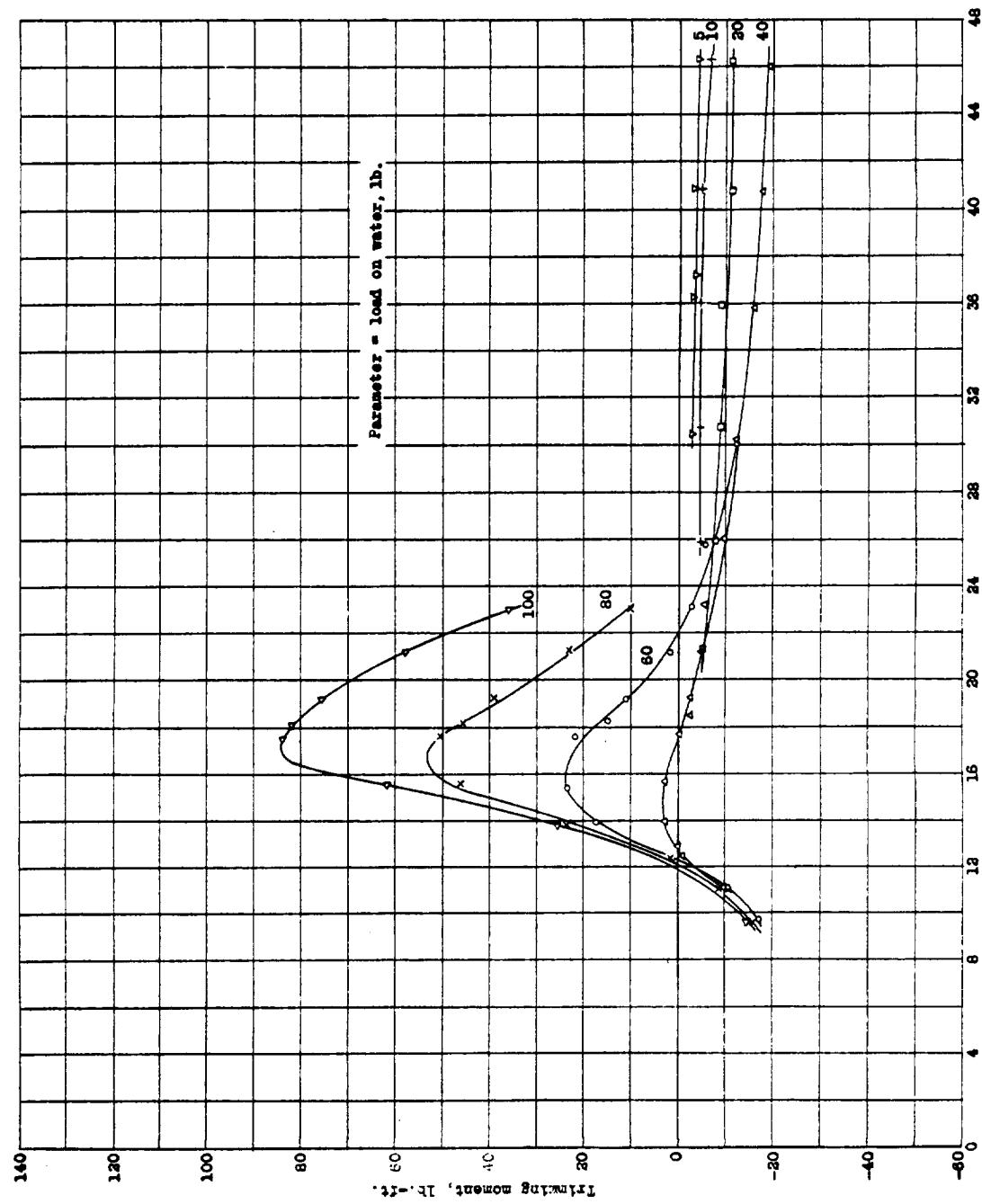
Resistance, lb.

Figure 19b.—Trimming moment. $\tau = 7°$. Model 11-C. ($5\frac{1}{2}°$ angle of afterbody keel)

Figure 20b.-Trimming moment. τ= 9°. Model 11-C.(5½° angle of after-
body keel.)
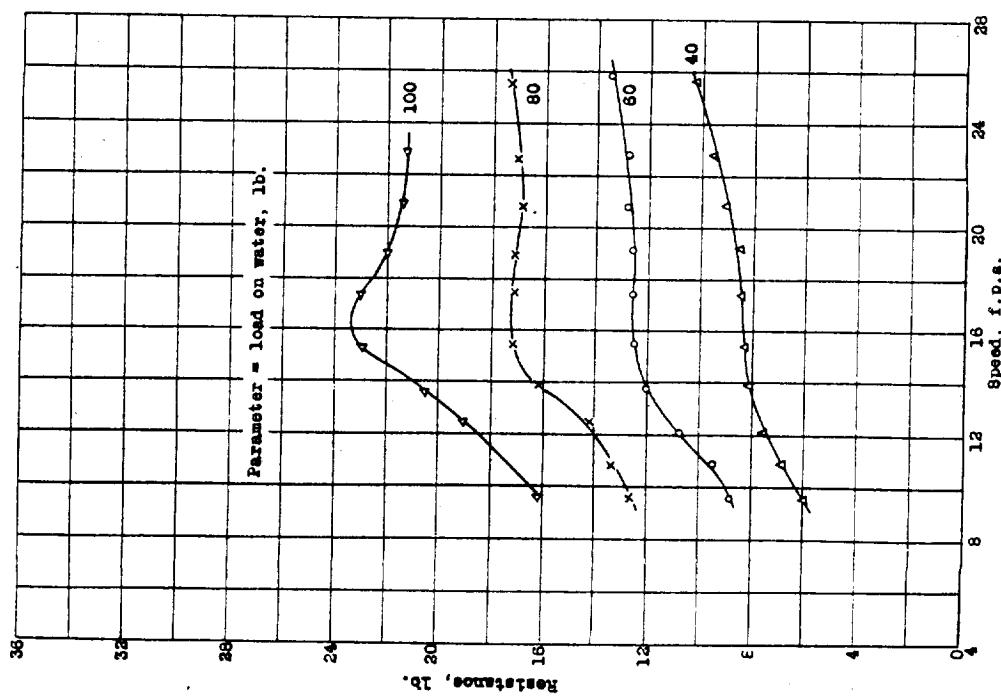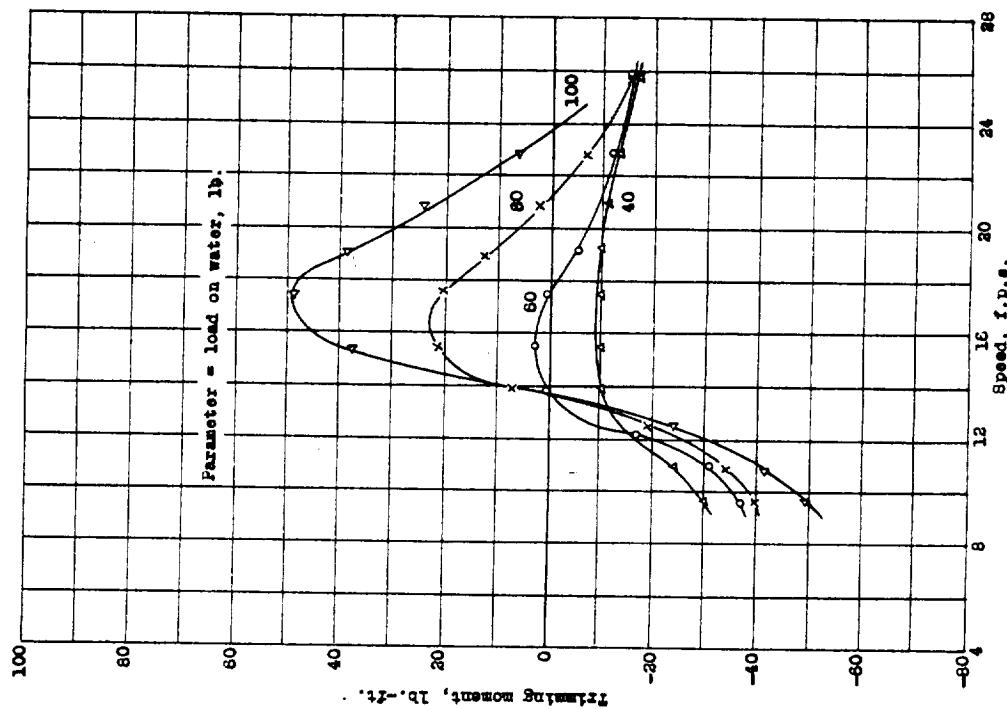
Figure 20 a.-Resistance. τ = 3°. Model 11-C.(5½° angle of afterbody keel)
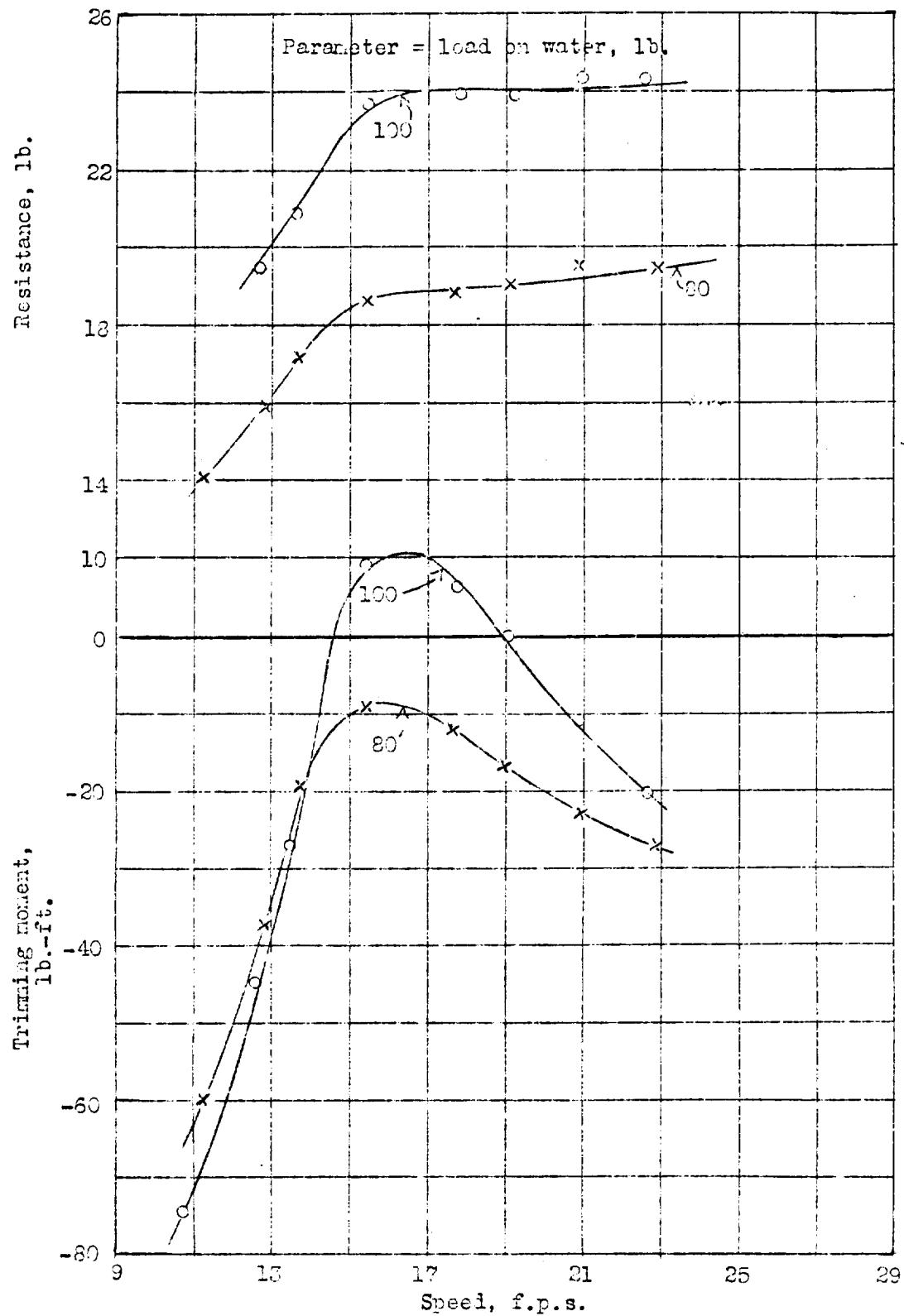
Figure 21.—Resistance and trimming moment, $\tau = 11°$. Model 11-C.
$5\tfrac{1}{2}°$ angle of afterbody keel

Figure 23.- Resistance and trimming moment, $\tau = 3°$. Model 11-0-9 (7° angle of afterbody keel)
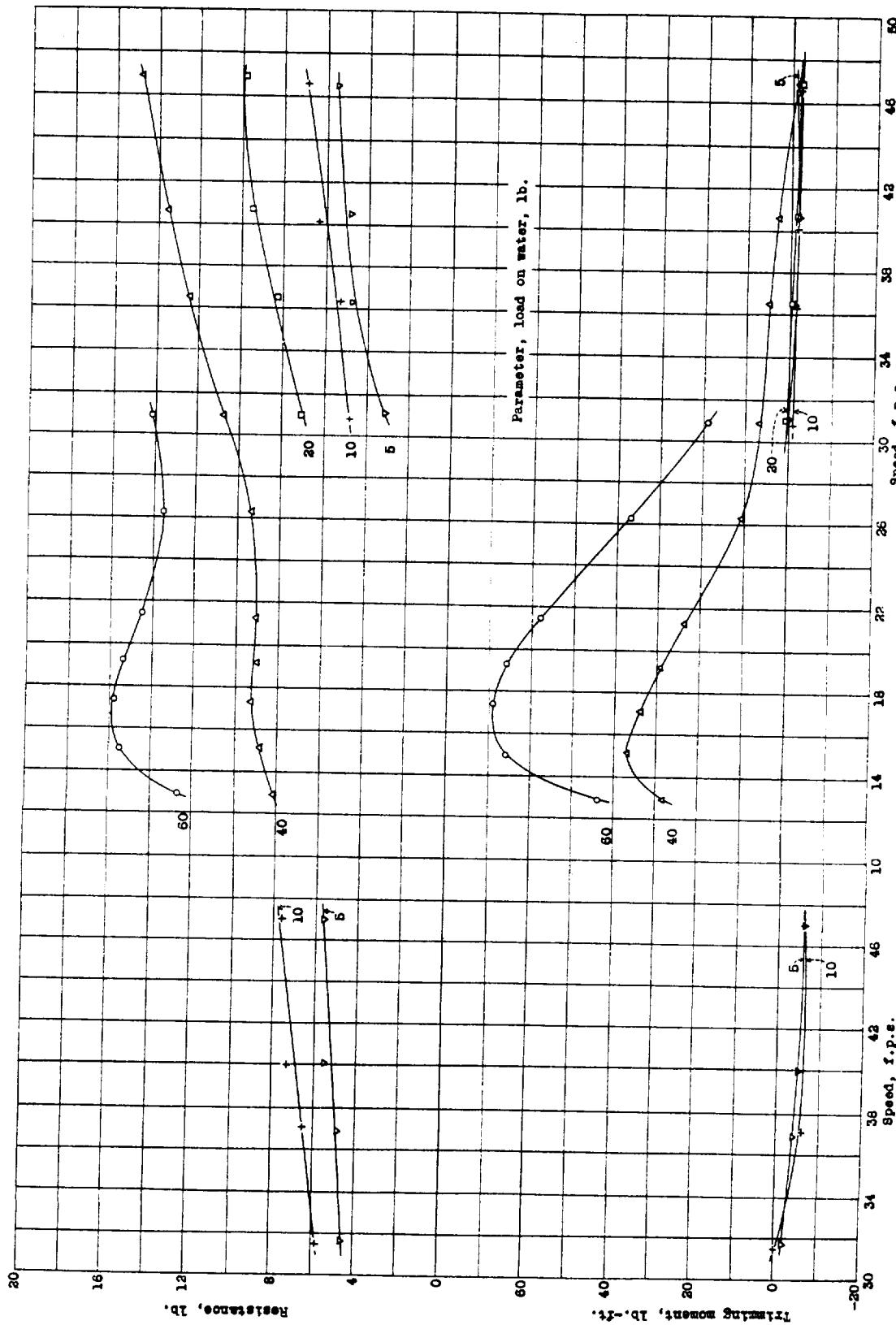
Figure 22.- Resistance and trimming moment, $\tau = 2°$. Model 11-0-9 (7° angle of afterbody keel)
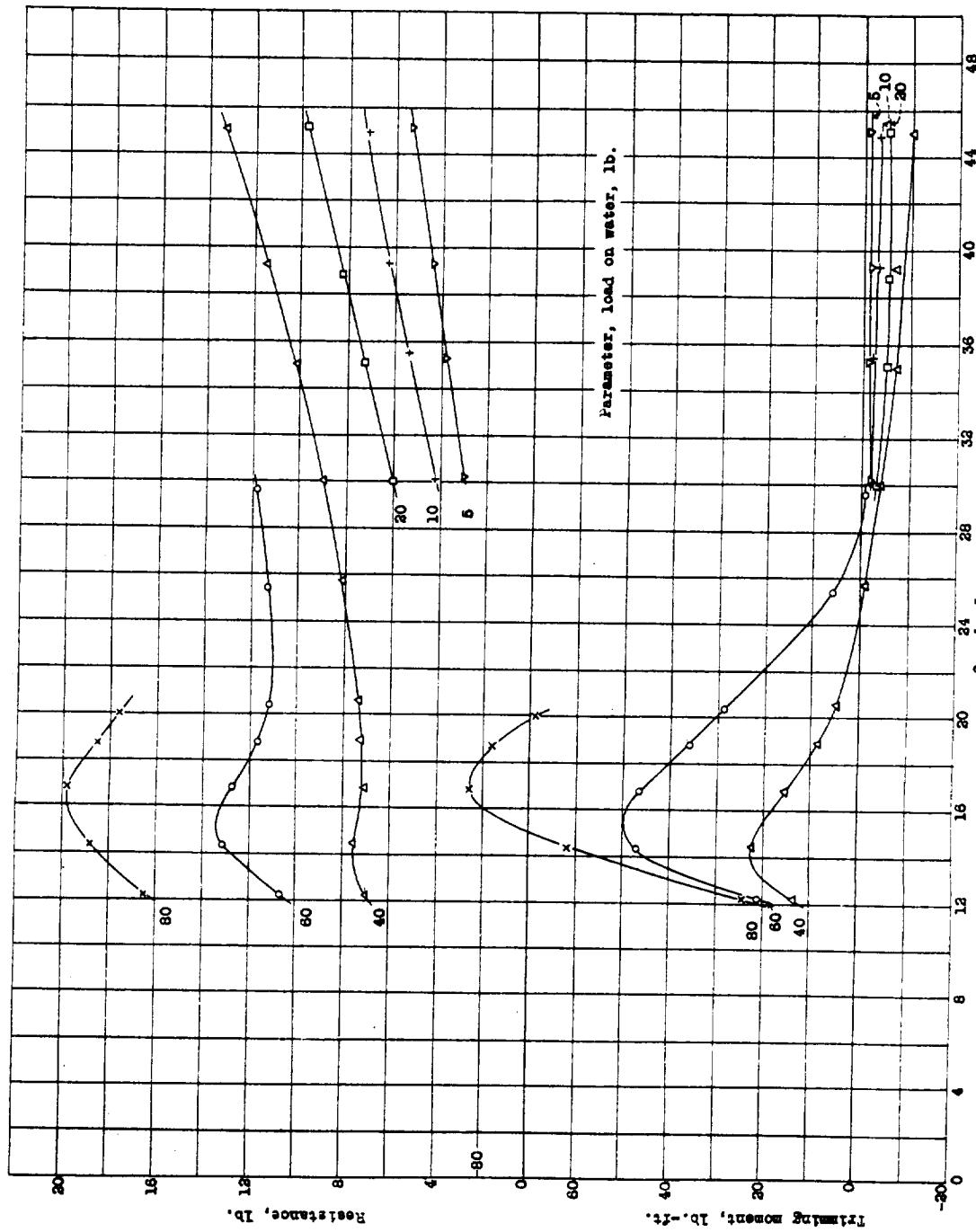
Figure 24.- Resistance and trimming moment, τ = 5°. Model 11-G-9 (7° angle of afterbody keel).

Fig. 25
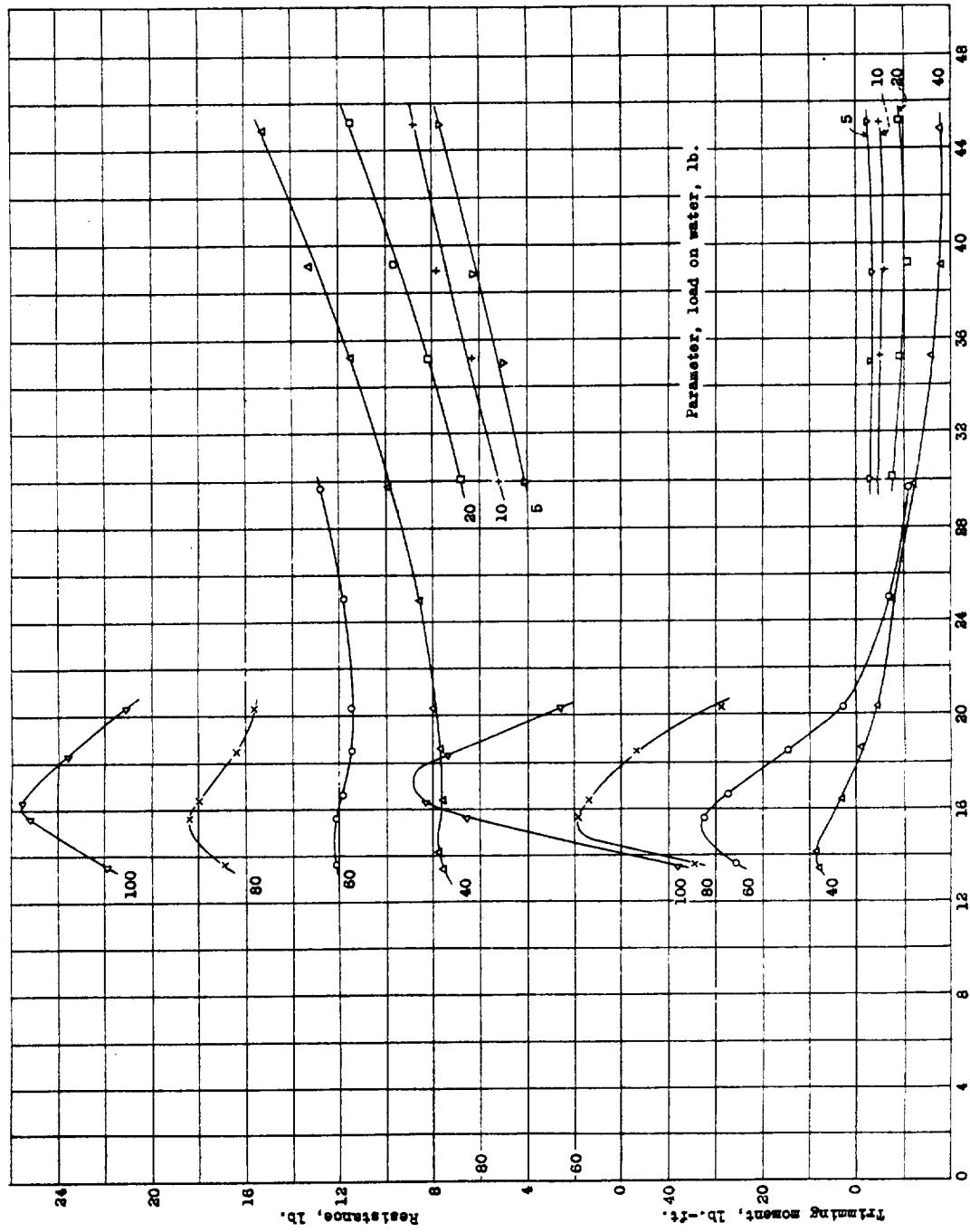
Figure 25.- Resistance and trimming moment, $\tau = 7°$. Model 11-C-9. ($7°$ angle of afterbody keel).
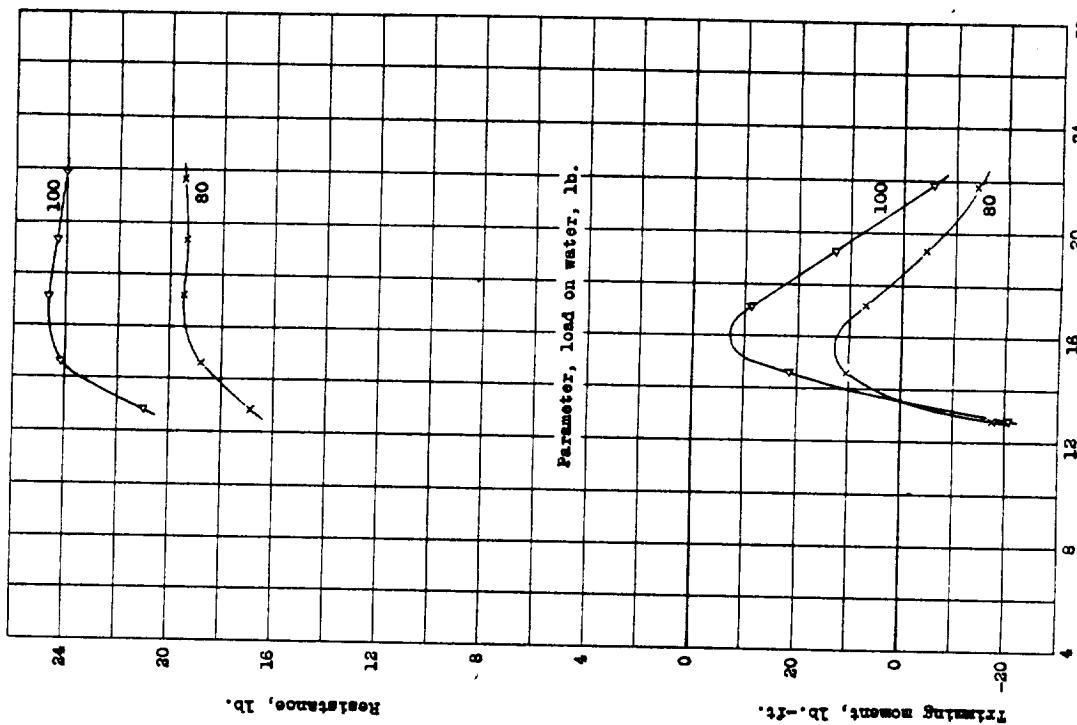
Figure 27.- Resistance and trimming moment, τ = 11°, Model 11-C-9 (7° angle of afterbody keel.)

Figure 26.- Resistance and trimming moment, τ = 9°, Model 11-C-8 (7° angle of afterbody keel.)

Figure 29.- Resistance and trimming moment, $\tau = 3°$. Model 11-C-10 (9° angle of afterbody keel).
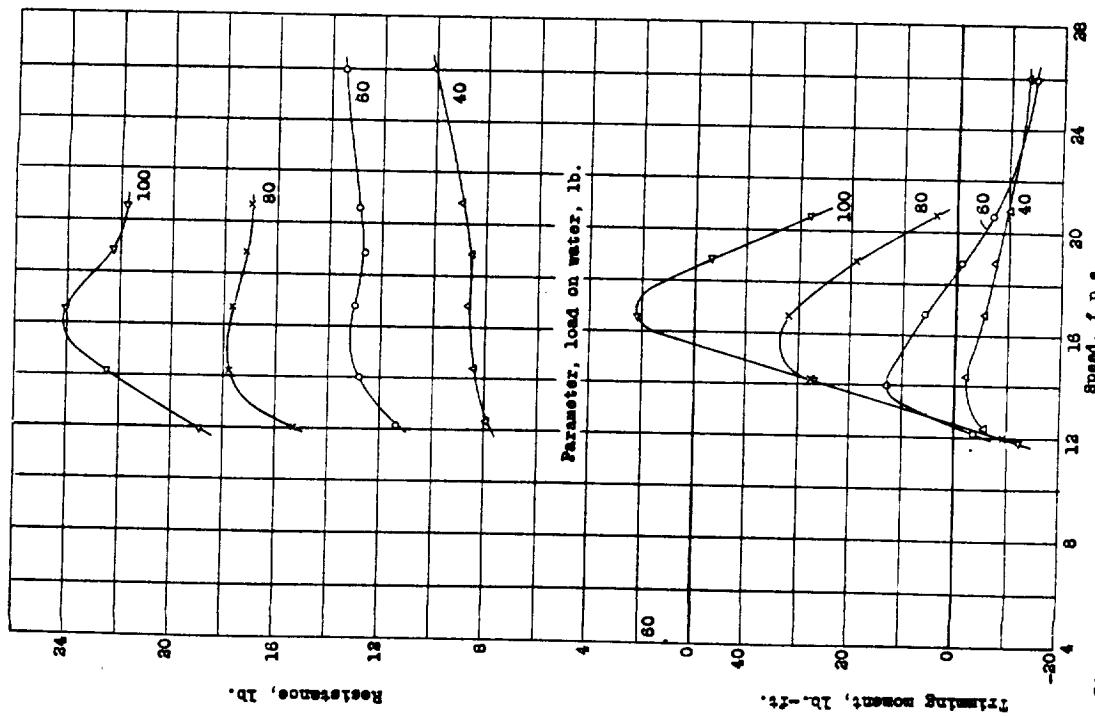
Figure 28.- Resistance and trimming moment, $\tau = 2°$. Model 11-C-10 (9° angle of afterbody keel).

Fig. 30
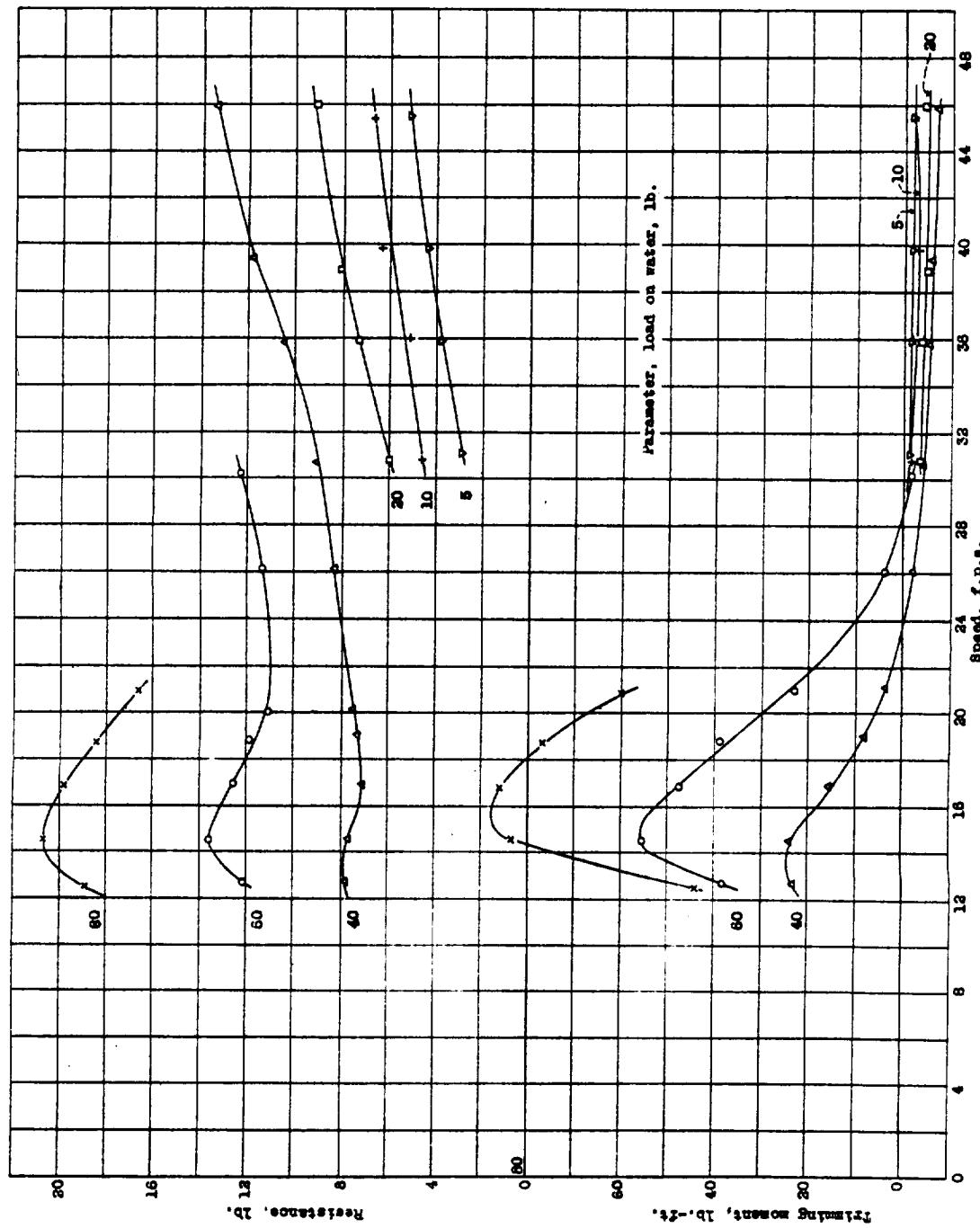
Figure 30.- Resistance and trimming moment, $\tau = 5°$. Model 11-G-10, (8° angle of afterbody keel)

Fig. 31
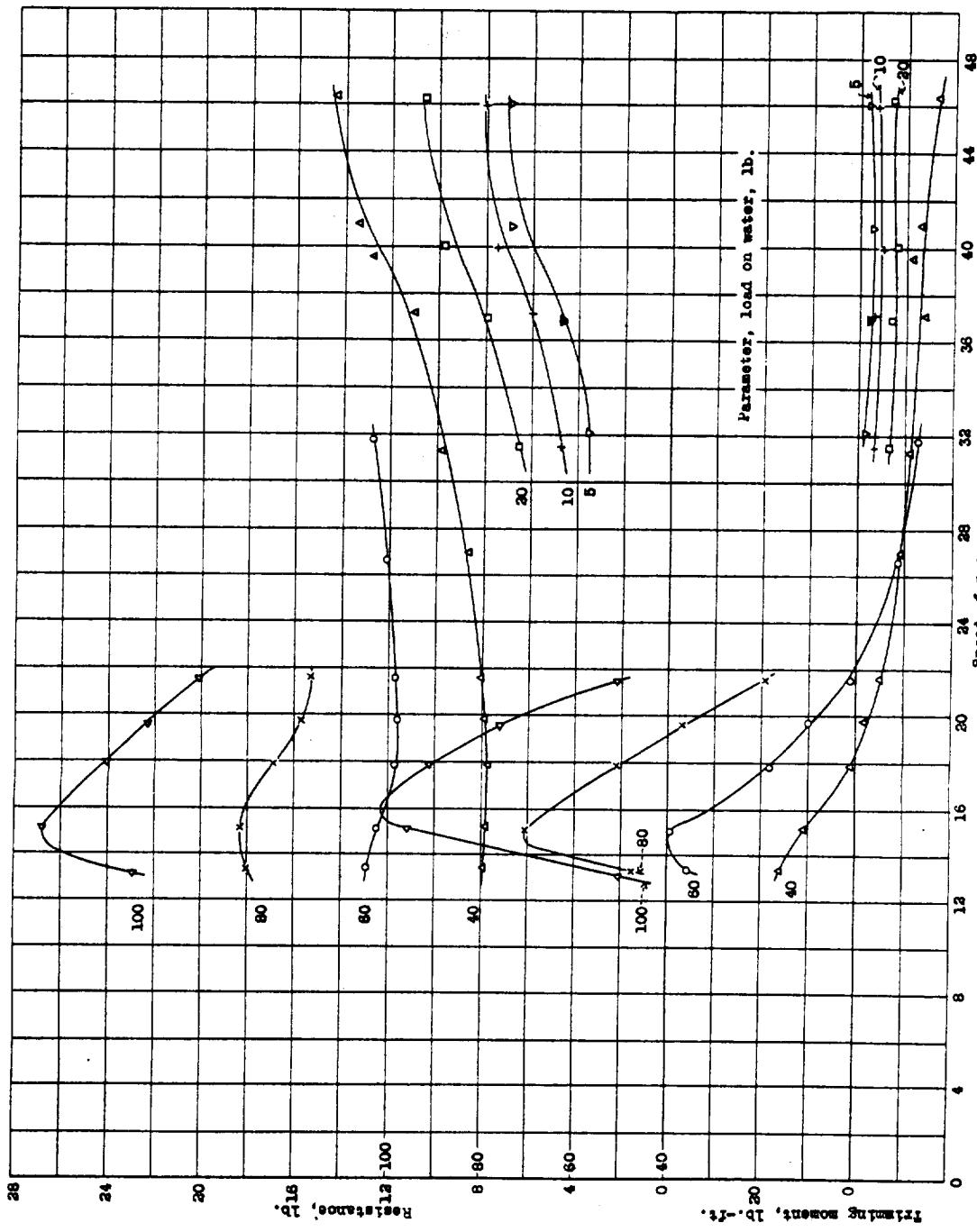
Figure 31.- Resistance and trimming moment, $\tau = 7^\circ$. Model 11-C-10 (9° angle of afterbody keel)

Figure 33. - Resistance and trimming moment, τ = 11°, Model 11-C-10
(9° angle of afterbody keel.)
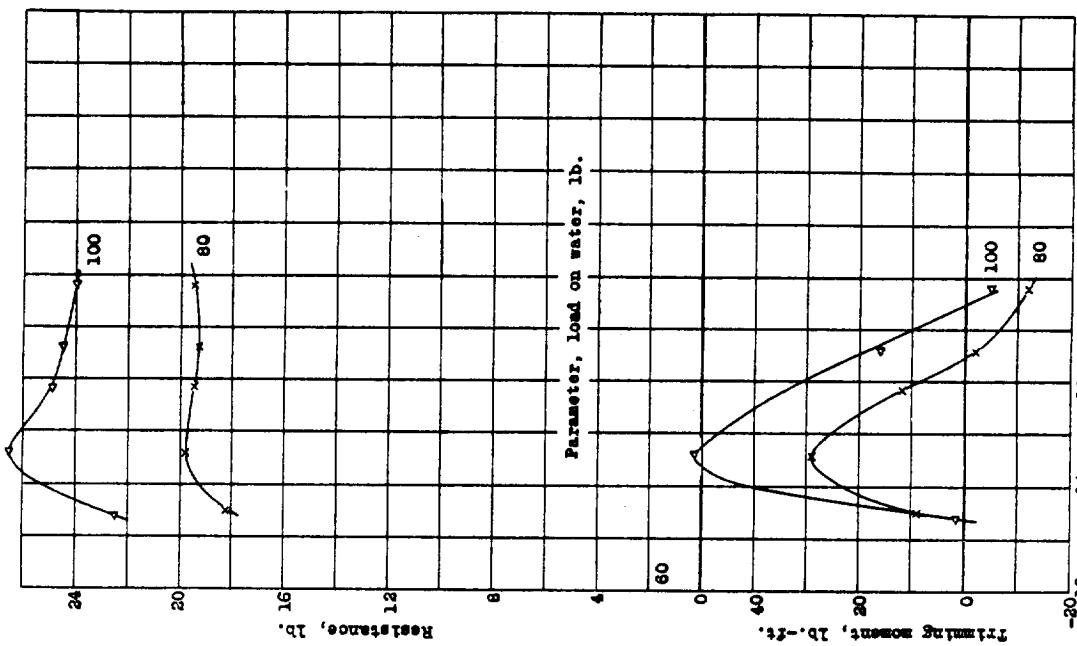
Figure 32.- Resistance and trimming moment, τ = 9°, Model 11-C-10
(9° angle of afterbody keel.)
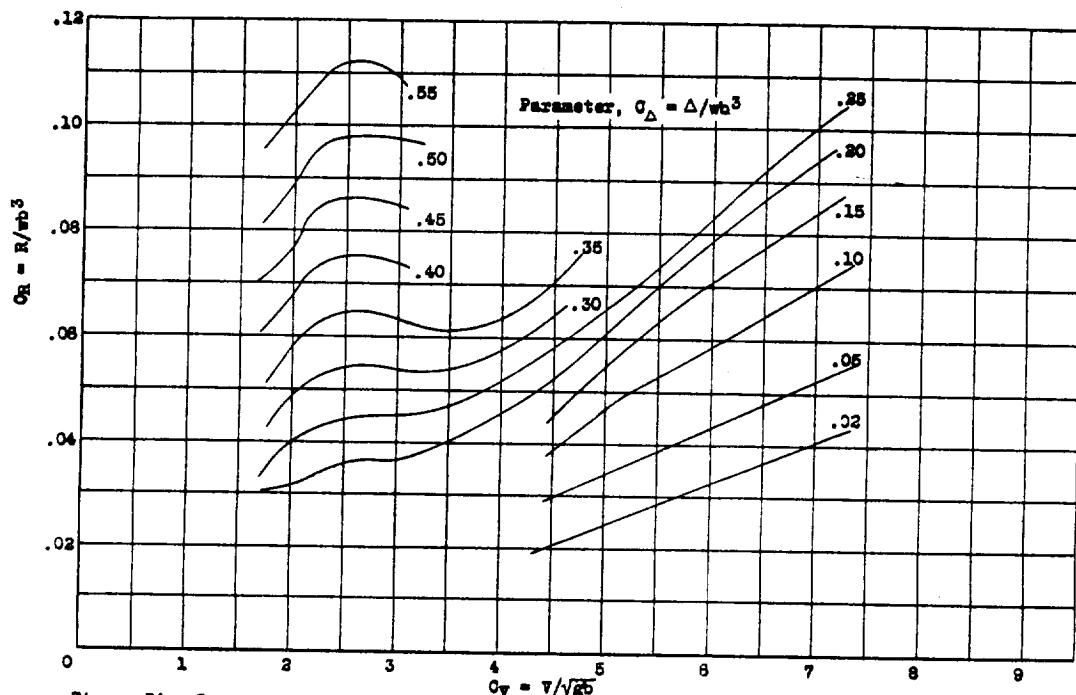
Figure 34.- Resistance coefficient at best trim angle, Model 11-C-7 (2-1/2° angle of afterbody keel.)
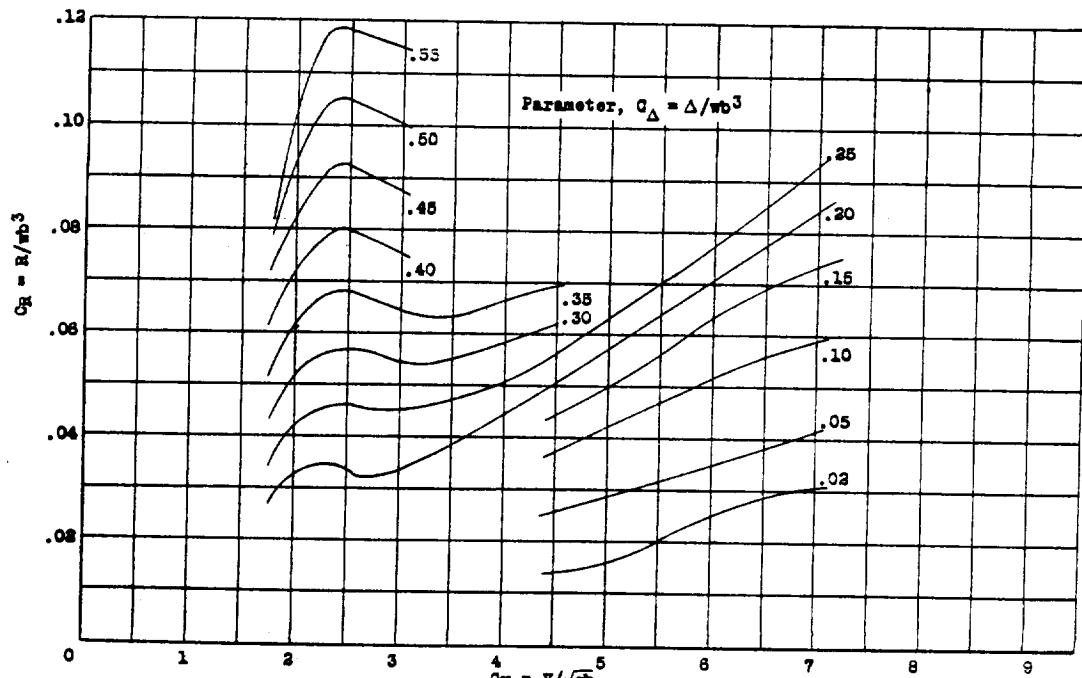
Figure 35.- Resistance coefficient at best trim angle, Model 11-C-8 (4° angle of afterbody keel.)
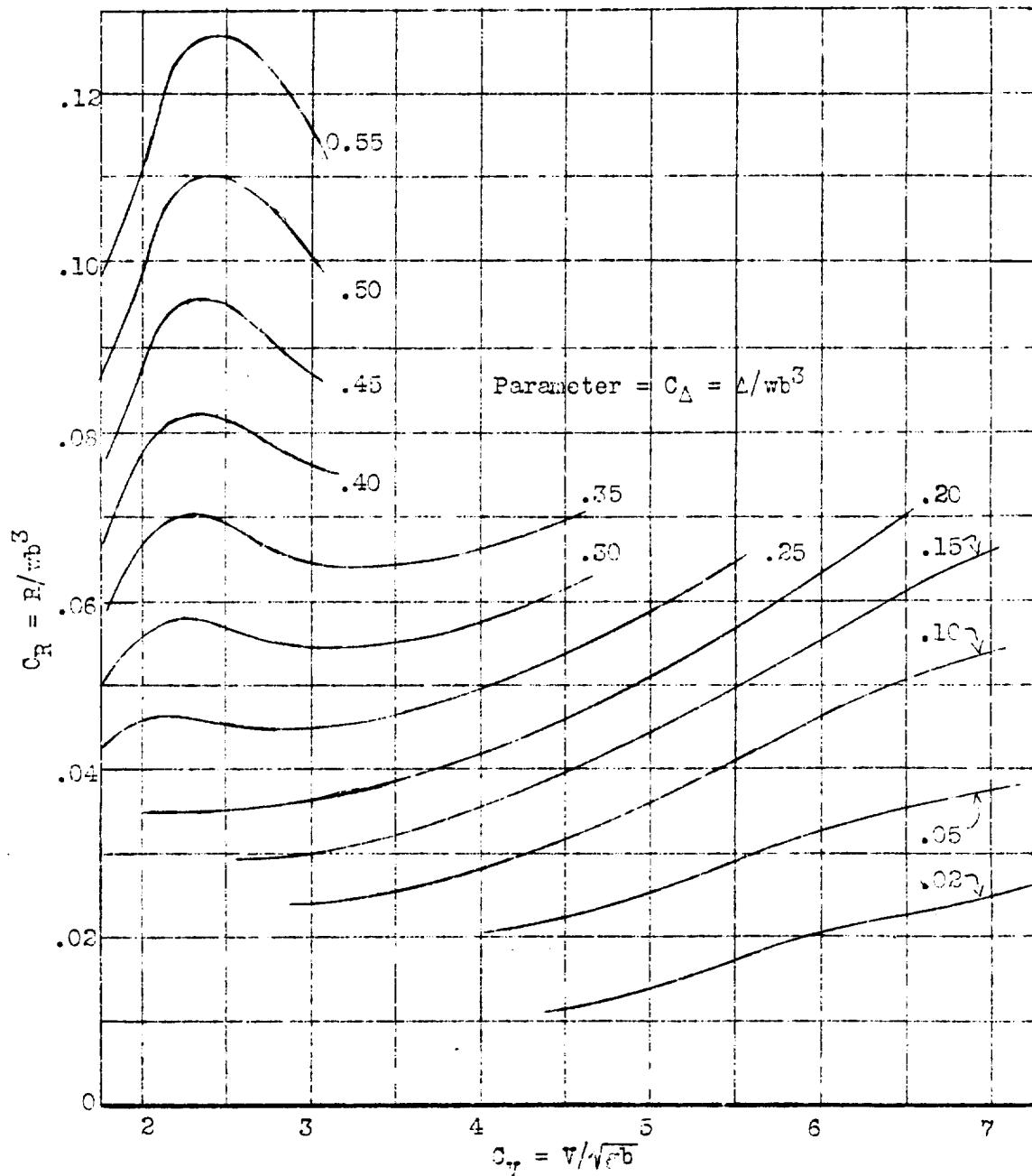
Figure 36.-Resistance coefficient at best trim angle. Model 11-C. (5 ½° angle of afterbody keel.)
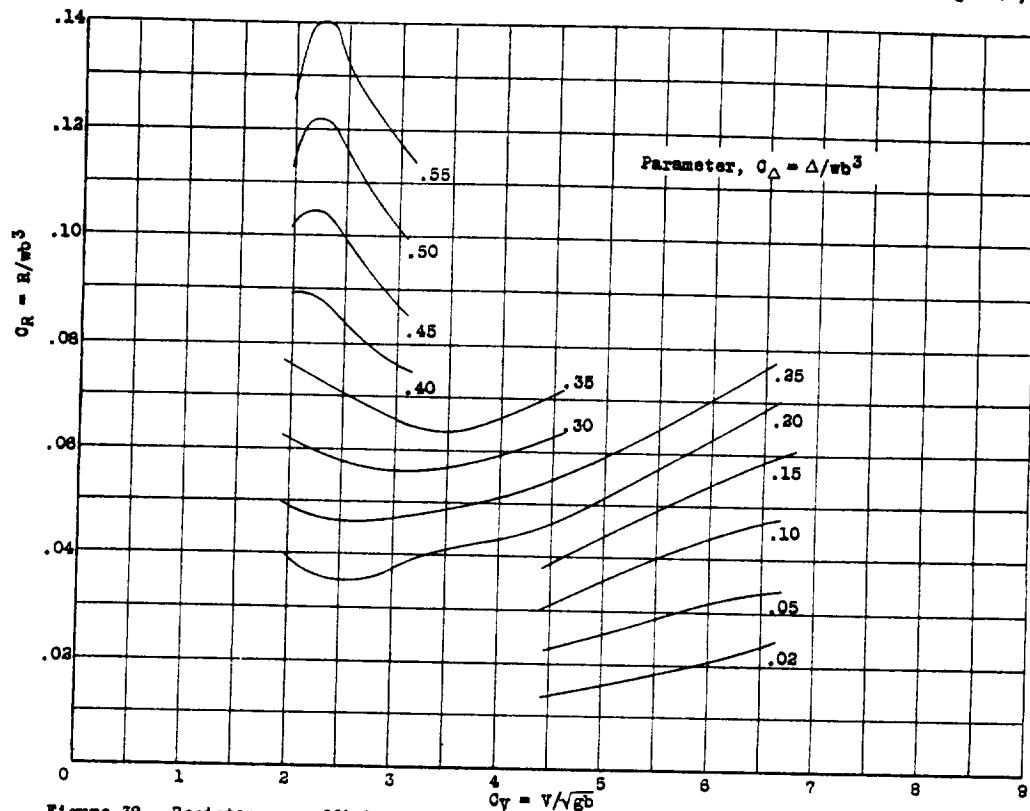
Figure 38.- Resistance coefficient at best trim angle, Model 11-C-10 (9° angle of afterbody keel.)
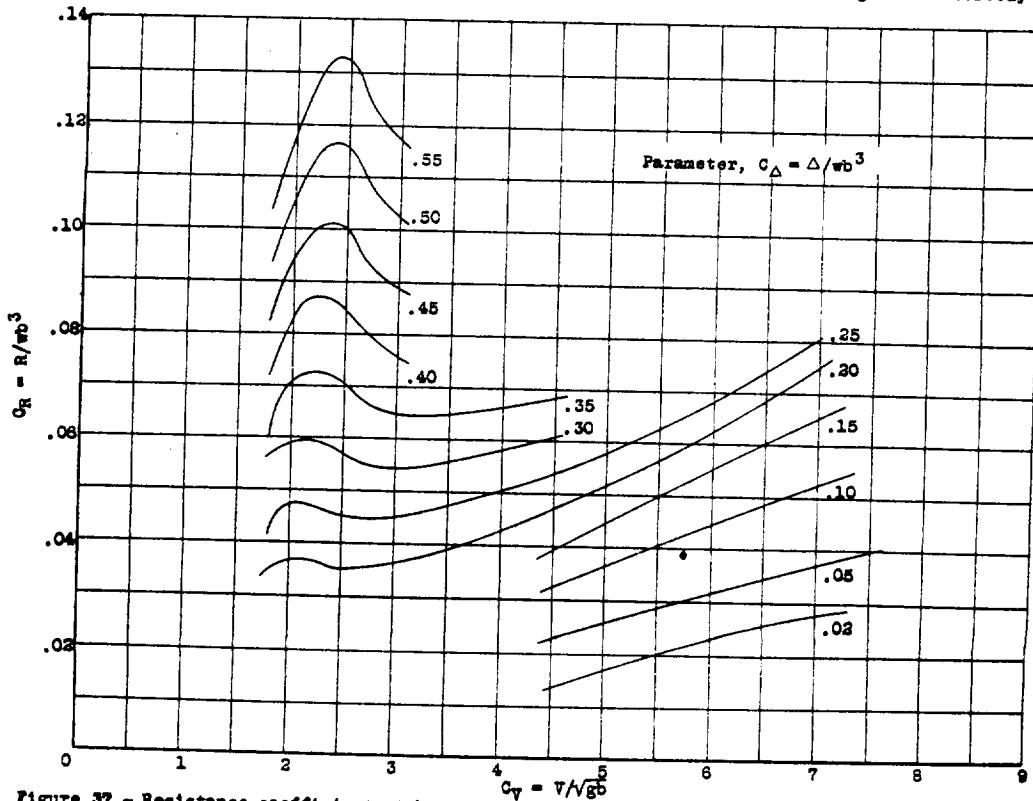
Figure 37.- Resistance coefficient at best trim angle, Model 11-C-9 (7° angle of afterbody keel.)
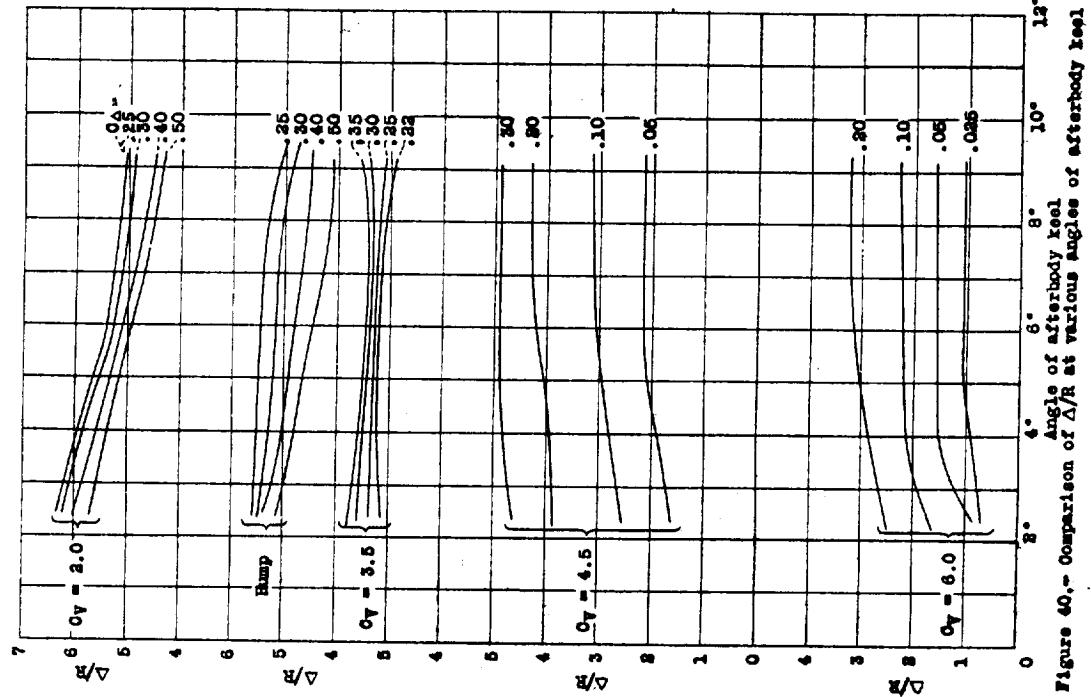
Figure 40.- Comparison of Δ/R at various angles of afterbody keel
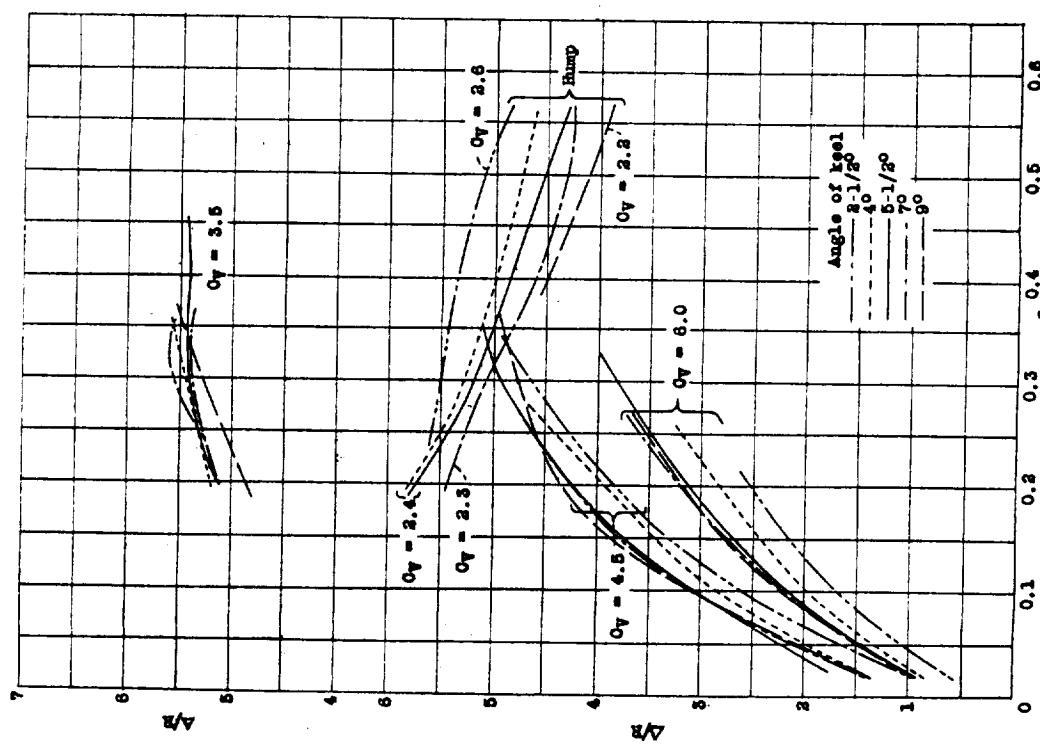
Figure 39.- Load / resistance ($C_Λ = Δ/R$) for various values of speed coefficient
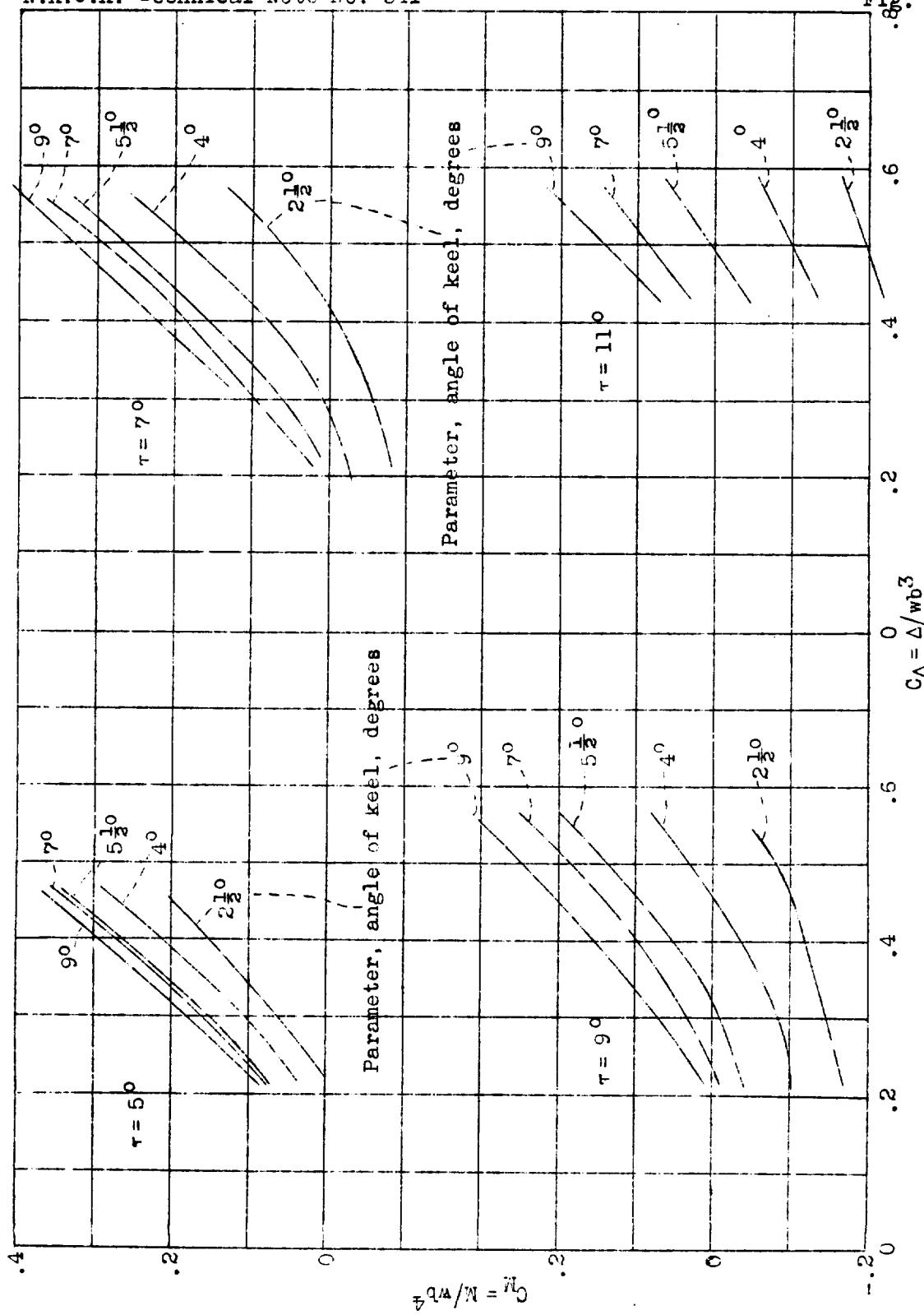
Figure 41.- Maximum trimming moment coefficient, positive direction.
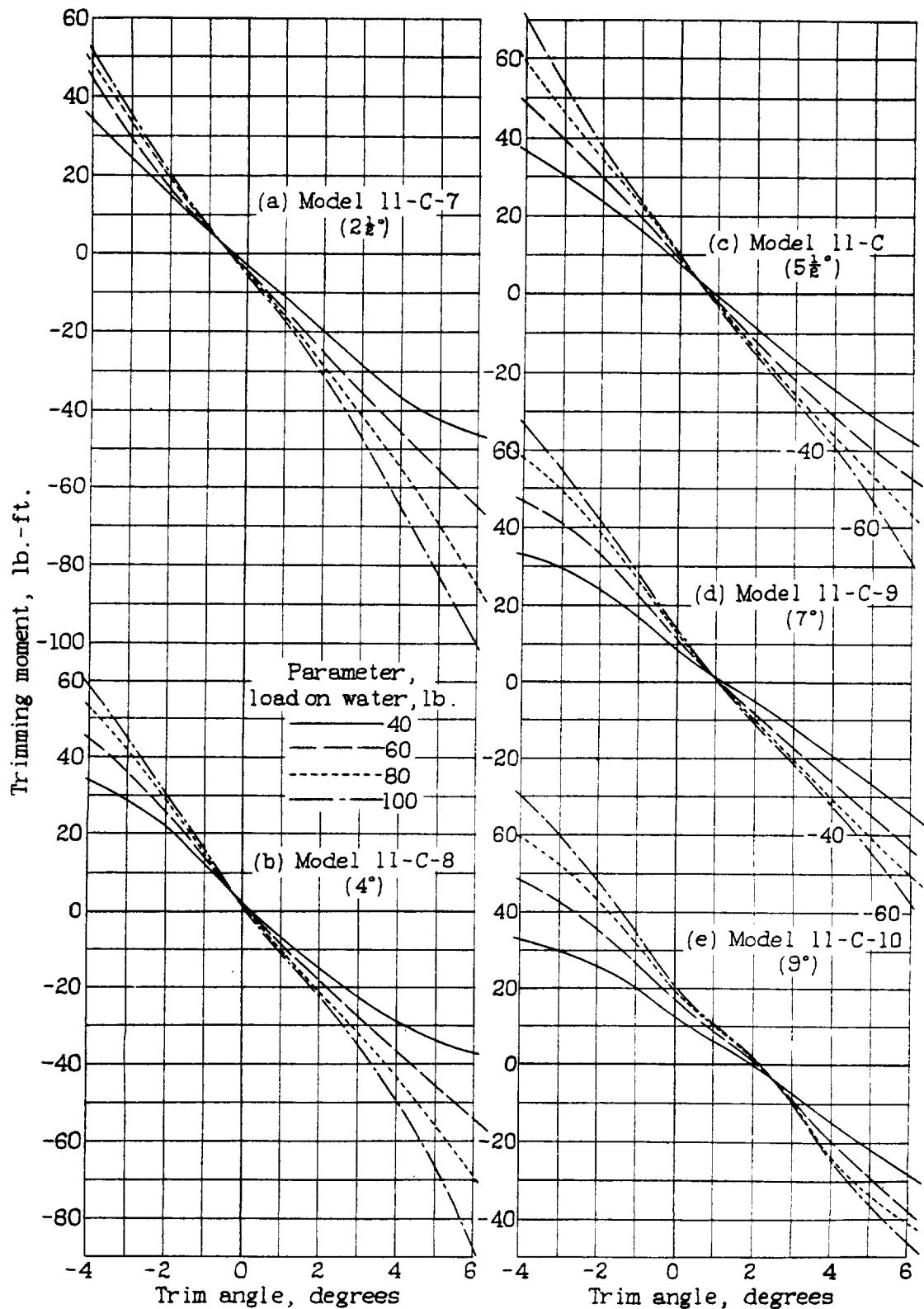
Figure 42.-Static trimming moments for various angles of afterbody keel.

Fig. 43
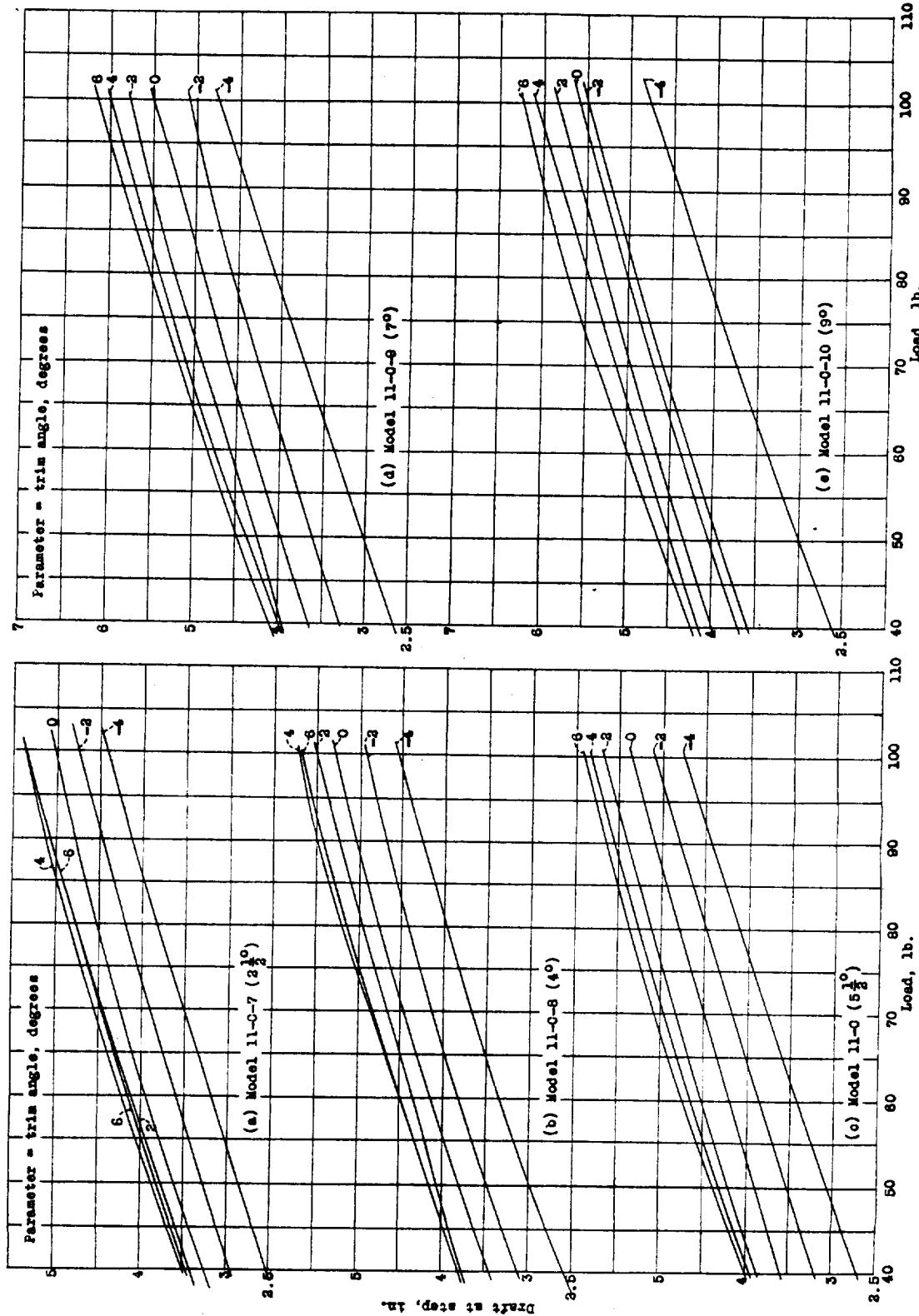
Figure 43.—Drafts at rest for various angles of afterbody keel.

Model 11-C-10
9° Angle of afterbody keel

Model 11-C-8
4° Angle of afterbody keel

(a) Load, 100 lb.,
speed, 12.8 f.p.s.
$\tau = 7°$

(b) Load, 100 lb.,
speed, 12.0 f.p.s.
$\tau = 7°$
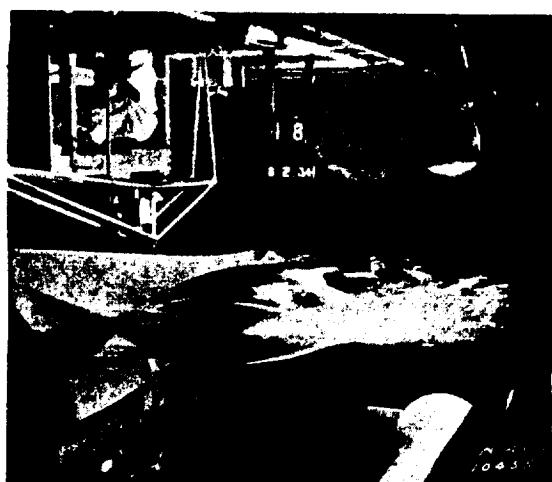
(c) Load, 100 lb.,
speed, 12.8 f.p.s.
$\tau = 7°$
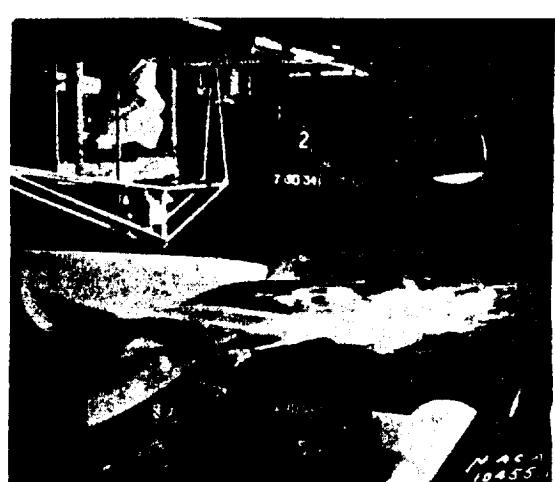
(d) Load, 100 lb.,
speed, 12.0 f.p.s.
$\tau = 7°$

Figure 44.- Photographs of spray

Model 11-C-10
9° Angle of afterbody keel

Model 11-C-3
4° Angle of afterbody keel

(a) Load, 40 lb.,
speed, 19.4 f.p.s.
$\tau = 9°$

(b) Load, 40 lb.,
speed, 20.0 f.p.s.
$\tau = 9°$
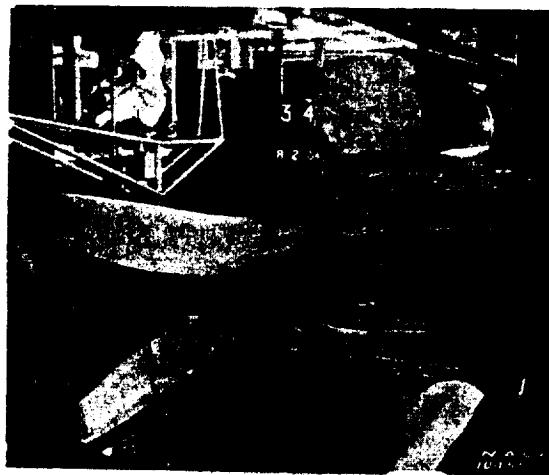
(c) Load, 40 lb.,
speed, 19.4 f.p.s.
$\tau = 9°$
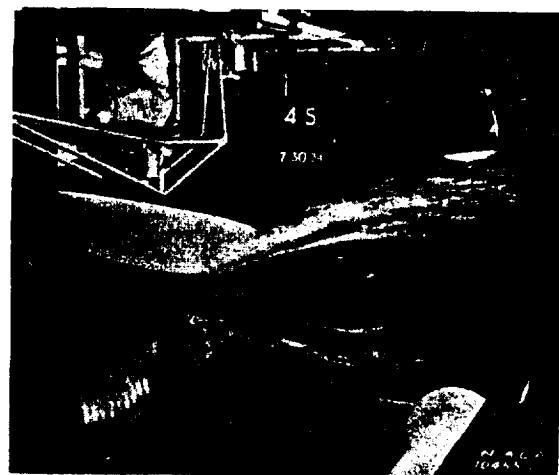
(d) Load, 40 lb.,
speed, 20.0 f.p.s.
$\tau = 9°$

Figure 45.- Photographs of spray

Fig. 46
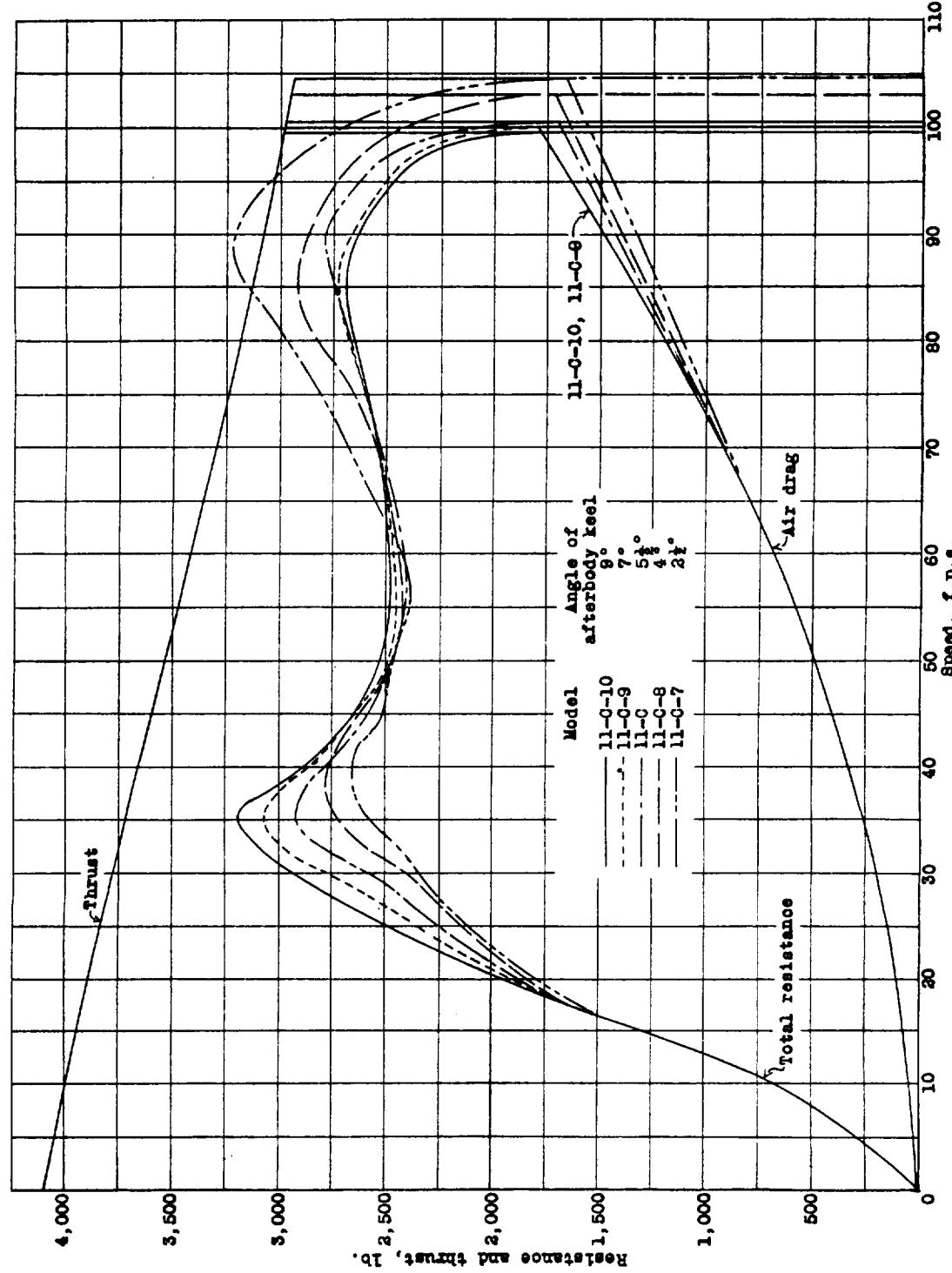
Figure 46.—Resistance and thrust of 15,000 lb. flying boat with various angles of afterbody keel.